



Measurement of the jet mass in high transverse momentum $Z(\rightarrow b\bar{b})\gamma$ production at $\sqrt{s} = 13$ TeV using the ATLAS detector



The ATLAS Collaboration*

ARTICLE INFO

Article history:

Received 17 July 2019

Received in revised form 27 November 2020

Accepted 30 November 2020

Available online 3 December 2020

Editor: M. Doser

ABSTRACT

The integrated fiducial cross-section and unfolded differential jet mass spectrum of high transverse momentum $Z \rightarrow b\bar{b}$ decays are measured in $Z\gamma$ events in proton–proton collisions at $\sqrt{s} = 13$ TeV. The data analysed were collected between 2015 and 2016 with the ATLAS detector at the Large Hadron Collider and correspond to an integrated luminosity of 36.1 fb^{-1} . Photons are required to have a transverse momentum $p_T > 175$ GeV. The $Z \rightarrow b\bar{b}$ decay is reconstructed using a jet with $p_T > 200$ GeV, found with the anti- k_r $R = 1.0$ jet algorithm, and groomed to remove soft and wide-angle radiation and to mitigate contributions from the underlying event and additional proton–proton collisions. Two different but related measurements are performed using two jet grooming definitions for reconstructing the $Z \rightarrow b\bar{b}$ decay: trimming and soft drop. These algorithms differ in their experimental and phenomenological implications regarding jet mass reconstruction and theoretical precision. To identify Z bosons, b -tagged $R = 0.2$ track-jets matched to the groomed large- R calorimeter jet are used as a proxy for the b -quarks. The signal yield is determined from fits of the data-driven background templates to the different jet mass distributions for the two grooming methods. Integrated fiducial cross-sections and unfolded jet mass spectra for each grooming method are compared with leading-order theoretical predictions. The results are found to be in good agreement with Standard Model expectations within the current statistical and systematic uncertainties.

© 2020 The Author. Published by Elsevier B.V. This is an open access article under the CC BY license (<http://creativecommons.org/licenses/by/4.0/>). Funded by SCOAP³.

Contents

1. Introduction	2
2. ATLAS detector	2
3. Data and Monte Carlo simulation	2
4. Event reconstruction and selection	3
5. Signal and background estimation	4
6. Definition of the observable and correction for detector effects	5
7. Systematic uncertainties	5
8. Results	7
8.1. Fit results and significance estimate	7
8.2. Integrated fiducial cross-section measurement	7
8.3. Differential fiducial cross-section measurement	7
9. Conclusion	7
Declaration of competing interest	9
Acknowledgements	9
References	9
The ATLAS Collaboration	11

* E-mail address: atlas.publications@cern.ch.

1. Introduction

This Letter presents a measurement of the fiducial and differential jet mass cross-sections of high transverse momentum (p_T) Z bosons that decay into $b\bar{b}$ pairs and are produced in association with a photon, denoted by $Z(\rightarrow b\bar{b})\gamma$. The analysis uses proton–proton (pp) collision data collected in 2015 and 2016 by the ATLAS detector [1] at the Large Hadron Collider (LHC) at a center-of-mass energy of $\sqrt{s} = 13$ TeV. This measurement of the unfolded jet mass spectrum of hadronically decaying Z bosons at the LHC explores the experimental features and phenomenological implications of techniques used to reconstruct boosted bosons – colour singlets – decaying into $b\bar{b}$. Similar measurements of gluons – colour octets – decaying into $b\bar{b}$ pairs have also been made by the ATLAS Collaboration [2]. The $Z(\rightarrow b\bar{b})\gamma$ process provides a well-defined experimental signature for measuring massive boosted Z bosons using high- p_T jets containing pairs of b -quarks. A detailed study of the $Z \rightarrow b\bar{b}$ signal is important for assessing systematic uncertainties and identification techniques for the measurement of $H \rightarrow b\bar{b}$ in the high- p_T range, as well as for potential TeV-scale resonances decaying into dibosons, one of them being a Z boson or a Higgs boson decaying into $b\bar{b}$ [3,4].

The $Z(\rightarrow b\bar{b})\gamma$ channel offers advantages in accessing the $Z \rightarrow b\bar{b}$ signal compared to the inclusive channels studied in Run 1 by ATLAS [5] and in Run 2 by CMS [6] since it provides both a useful trigger signature via the photon and an opportunity to directly estimate background processes using the data. Initial results of the modelling of jet kinematics in the $Z(\rightarrow b\bar{b})\gamma$ channel using 13 TeV data collected by ATLAS are presented in Ref. [7]. The measurement described in this Letter selects $b\bar{b}$ decays of a Z boson contained within a single jet, referred to as a Z -jet, with transverse momentum $p_T^{Z\text{-jet}} > 200$ GeV and a photon with transverse momentum $p_T^\gamma > 175$ GeV. The high- p_T requirement enhances the signal over the dominant γ + jets background production, which has a softer p_T spectrum. The candidate Z -jet is reconstructed using a ‘groomed’ anti- k_r [8] jet with radius parameter $R = 1.0$ (large- R jet). A multivariate algorithm is used to determine whether $R = 0.2$ track-jets that are associated with the large- R jet are b -tagged, i.e. if they contain b -hadron decay products. The approach to tagging presented in this Letter is built upon a foundation of studies from LHC runs at $\sqrt{s} = 7$ and 8 TeV, including extensive studies of jet reconstruction and grooming algorithms [9–11] and detailed investigations of track-jet-based b -tagging in boosted topologies [7,12].

Two different jet grooming algorithms are used to perform the measurement: ‘trimming’ [10], and ‘soft drop’ [11,13]. The experimental and phenomenological implications for jet mass reconstruction and theoretical precision are different for the two grooming algorithms. The trimming algorithm is the default used in ATLAS to study boosted bosons, chosen as a result of optimisation studies performed from LHC runs at $\sqrt{s} = 8$ and 13 TeV [14]. The soft-drop calculations achieve a different theoretical precision and offer advantages such as the formal absence of non-global logarithms. The distribution of the soft-drop mass for QCD processes has now been calculated both at next-to-leading order (NLO) with next-to-leading-logarithm (NLL) accuracy [15,16] and at leading order (LO) with next-to-next-to-leading-logarithm (NNLL) accuracy [17,18]. This level of precision for a jet substructure observable at a hadron collider is surpassed only by the calculation of thrust in e^+e^- interactions [19]. Similar calculations are not currently available for trimmed jets.

The double differential cross-section of soft-drop jets as a function of the mass and transverse momentum were previously measured by ATLAS [20] and CMS [21] in balanced dijet events at $\sqrt{s} = 13$ TeV. The trimmed jet mass distribution in dijet and W/Z +jets events was measured by CMS at $\sqrt{s} = 7$ TeV [22]. While previous

analyses measured the cross-section of quark and gluon-initiated jets for different grooming algorithms, this analyses measures the mass of large- R jets containing the hadronic decay products of Z bosons in $Z(\rightarrow b\bar{b})\gamma$ events at $\sqrt{s} = 13$ TeV.

2. ATLAS detector

The ATLAS detector at the LHC is a multipurpose particle detector with a forward–backward symmetric cylindrical geometry and a near 4π coverage in solid angle.¹ It consists of an inner detector (ID) for tracking surrounded by a thin superconducting solenoid providing a 2 T axial magnetic field, electromagnetic and hadronic calorimeters, and a muon spectrometer. The ID covers the pseudorapidity range $|\eta| < 2.5$. It consists of silicon pixel, silicon microstrip, and transition radiation tracking detectors. A new inner pixel layer, the insertable B-layer [23,24], was added at a mean radius of 3.3 cm during the period between Run 1 and Run 2 of the LHC. Lead/liquid-argon (LAr) sampling calorimeters provide electromagnetic (EM) energy measurements with high granularity ($|\eta| < 3.2$). The hadronic calorimeter uses a steel/scintillator-tile sampling detector in the central pseudorapidity range ($|\eta| < 1.7$) and a copper/LAr detector in the region $1.5 < |\eta| < 3.2$. The forward regions ($3.2 < |\eta| < 4.9$) are instrumented with copper/LAr and tungsten/LAr calorimeter modules optimised for electromagnetic and hadronic measurements, respectively. A muon spectrometer with an air-core toroid magnet system surrounds the calorimeters. Three layers of high-precision tracking chambers provide coverage in the range $|\eta| < 2.7$, while dedicated fast chambers allow triggering in the region $|\eta| < 2.4$. The ATLAS trigger system consists of a hardware-based first-level trigger followed by a software-based high-level trigger [25].

3. Data and Monte Carlo simulation

The data were collected in pp collisions at the LHC with $\sqrt{s} = 13$ TeV and a 25 ns proton bunch crossing interval during 2015 and 2016. The full data sample corresponds to an integrated luminosity of 36.1 fb^{-1} after requiring that all detector subsystems were operational during data recording. The uncertainty in the combined 2015–2016 integrated luminosity is 2.1% [26], obtained using the LUCID-2 detector [27] for the primary luminosity measurements. Collision events were recorded with a trigger selecting events with at least one photon candidate with transverse energy $E_T > 140$ GeV.

Monte Carlo (MC) event samples that include an ATLAS detector simulation [28] based on GEANT 4 [29] are used to model the $Z\gamma$ signal and the small $t\bar{t} + \gamma$ and $W\gamma$ background contributions. In addition, γ + jets MC event samples are used to study the trigger modelling. In addition to the hard scatter, each event was overlaid with additional pp collisions (pile-up) according to the distribution of the average number of pp interactions per bunch crossing, $\langle \mu \rangle$, observed in data. These additional pp collisions were generated with PYTHIA 8.1 [30] using the ATLAS A2 set of tuned parameters [31] and the NNPDF23LO [32] parton distribution function (PDF) set. Simulated events were then reconstructed with the same algorithms as those run on collision data.

¹ ATLAS uses a right-handed coordinate system with its origin at the nominal interaction point in the centre of the detector. The positive x -axis is defined by the direction from the interaction point to the centre of the LHC ring, with the positive y -axis pointing upwards, while the beam direction defines the z -axis. Cylindrical coordinates (r, ϕ) are used in the transverse plane, ϕ being the azimuthal angle around the z -axis. The pseudorapidity η is defined in terms of the polar angle θ by $\eta = -\ln \tan(\theta/2)$. Rapidity is defined as $y = 0.5 \ln[(E + p_z)/(E - p_z)]$ where E denotes the energy and p_z is the component of the momentum along the beam direction. The angular distance ΔR is defined as $\sqrt{(\Delta y)^2 + (\Delta \phi)^2}$.

The $Z\gamma$ signal was modelled using the LO SHERPA 2.1.1 [33] generator, with the CT10 NLO [34] PDF set; the sample is flavour inclusive ($Z(\rightarrow qq)\gamma$). An alternative $Z\gamma$ sample was produced with MADGRAPH 5.2 [35], which generated LO matrix elements that were then parton showered with PYTHIA 8.1 using the NNPDF23LO PDF set and the ATLAS A14 set of tuned parameters [36] for the underlying event. This alternative signal sample is used to determine the systematic uncertainty associated with the signal modelling.

The γ + jets samples were also generated with SHERPA 2.1.1 and the CT10 NLO PDF set. The matrix element was configured to allow a photon with up to three partons in the final state. The $t\bar{t} + \gamma$ processes were modelled by MADGRAPH 5.2 interfaced to PYTHIA 8.1. NLO corrections were applied to the $t\bar{t} + \gamma$ cross-section [37]. The $W\gamma$ MC samples with hadronically decaying W bosons were generated using SHERPA 2.1.1, with a configuration similar to that used for the $Z\gamma$ sample. Predictions for $W\gamma$ production were normalised according to the cross-sections provided by the generator.

4. Event reconstruction and selection

Events are required to have a reconstructed primary vertex, defined as the vertex with at least two reconstructed tracks with $p_T > 0.4$ GeV and with the highest sum of squared transverse momenta of associated tracks [38].

Hadronically decaying high- p_T $Z \rightarrow b\bar{b}$ candidates are identified using large- R jets to capture both b -quarks, since they will be very close due to the high Lorentz boost. The two different jet grooming algorithms considered in the analysis, trimming and soft drop, differ in their pile-up mitigation and mass resolution performance.

Trimmed calorimeter jets Trimmed calorimeter jets are reconstructed from noise-suppressed topological clusters (topoclusters) of calorimeter energy deposits calibrated to the local hadronic scale (LC) [39], using the anti- k_t algorithm with radius parameter $R = 1.0$ implemented in FASTJET [40,41]. Trimmed calorimeter jets are those jets to which the trimming algorithm [10] is applied. The aim of this algorithm is to improve the jet mass resolution and its stability with respect to pile-up by discarding the softer components of jets that originate from initial-state radiation, pile-up interactions, or the underlying event. This is done by reclustering the constituents of the initial large- R jet, using the k_t algorithm [42,43], into subjets with radius parameter $R_{\text{sub}} = 0.2$ and removing any subjet that has a p_T less than 5% (f_{cut}) of the parent jet p_T . The jet mass m^{jet} , the main observable in this analysis, is defined as the magnitude of the four-momentum sum of constituents inside a jet. It is referred to as the calorimeter-based mass if it is calculated using the topoclusters as constituents, or as the track-assisted jet mass [44] if it is estimated by using tracking information. The jet mass for trimmed jets is defined as the weighted combination of the calorimeter-based mass and the track-assisted jet mass [44], where each input mass is weighted by a factor proportional to their inverse-squared mass resolution.

Soft-drop calorimeter jets Soft-drop calorimeter jets are formed by the application of the soft-drop algorithm [11] to the anti- k_t $R = 1.0$ jets described above, with additional topological cluster preprocessing that is described below. The soft-drop algorithm is designed to remove soft and wide-angle radiation and also contamination from pile-up. In the first step of the grooming algorithm, the anti- k_t $R = 1.0$ jets are reclustered with the Cambridge-Aachen (C/A) [45,46] algorithm so that the constituents are combined purely according to their angular separation. The soft-drop algorithm then reverses the C/A algorithm clustering history and removes the softer subjet at a specific step of the C/A clustering history unless the soft-drop condition is fulfilled:

$$\frac{\min(p_{T1}, p_{T2})}{p_{T1} + p_{T2}} > z_{\text{cut}} \left(\frac{\Delta R_{12}}{R_0} \right)^\beta,$$

where z_{cut} and β are algorithm parameters, p_{T1} and p_{T2} are the transverse momenta of the declustered subjets at each history step, ΔR_{12} is the distance between the subjets in the (η, ϕ) space and R_0 is a threshold corresponding to the jet radius. The parameters $\beta = 0$ and $z_{\text{cut}} = 0.1$ are used in the analysis, based on the studies in Ref. [47]. The final measurement is performed for jet mass $m^{\text{jet}} > 30$ GeV, which implies that any collinear divergence is regulated and the measurement remains protected against collinear singularities. The soft-drop jet mass exhibits a pile-up dependence with the chosen parameters and therefore a special version of pile-up suppressed topological clusters are used to construct the jets that are then groomed with the soft-drop algorithm. Specifically, the SoftKiller (SK) algorithm [48] is used in conjunction with Constituent Subtraction (CS) [49,50] based on the studies presented in Ref. [47]. CS is applied before the SK algorithm. The CS is an extension of the pile-up subtraction based on jet area [51]. The algorithm proceeds as follows. First, virtual particles with infinitesimally small p_T (ghosts) are added to the event (each covering a fixed area in the η - ϕ plane) with energy density matching the median energy density of the event. Second, the added ghosts are matched to the topological clusters in η - ϕ space and only those within $\Delta R = 0.25$ of the topocluster are further considered for the pile-up removal procedure. The algorithm proceeds then iteratively through each topocluster-ghost pair in order of ascending ΔR . If the p_T of the topocluster is larger than that of the matched ghost, the p_T of the individual topocluster is corrected by subtracting the p_T of the ghost and the ghost are removed. Otherwise the p_T of the topocluster is subtracted from the p_T of the ghost and the p_T of the topocluster is set to zero. The SK algorithm exploits the characteristic that particles originating from pile-up collisions are softer than those from the hard-scattering collision and removes particles that fall below a certain p_T threshold, determined on an event-by-event basis. The pile-up suppressed topological clusters after CS and SK are used as input to the soft-drop jet reconstruction. The calorimeter-based jet mass is used for soft-drop jets.

All groomed jets A dedicated MC-based calibration, similar to the procedure used in Ref. [44], is applied to correct the jet p_T and mass of both the trimmed jets and the soft-drop jets to the particle level. To account for semileptonic decays of the b -hadrons, the four-momentum of the closest reconstructed muon candidate within $\Delta R = 0.2$ of the b -tagged track-jet is taken into account in the calorimeter-based component of the jet mass observable (see below for the description of the track-jet definition and b -tagging). Muon candidates are identified by matching ID tracks to full tracks or track segments reconstructed in the muon spectrometer. Muons are required to have $p_T > 10$ GeV and $|\eta| < 2.4$, and to satisfy the loose identification criteria of Ref. [52], which impose quality requirements on the tracks, but no isolation criteria are applied. A calibration is applied to correct the muon transverse momentum, and reconstruction and identification efficiency scale factors, derived from $J/\psi \rightarrow \mu^+\mu^-$ and $Z \rightarrow \mu^+\mu^-$ events [52], are applied to simulation. Large- R jets are required to have $p_T > 200$ GeV and $|\eta| < 2.0$. A comparison of the calibrated Z -jet mass distribution and the particle-level jet mass distribution for trimmed jets and soft-drop jets is shown in Fig. 1. Particle-level jets, used in the unfolding procedure described in Section 6, are built from stable final-state particles (defined as those with proper lifetime τ corresponding to $c\tau > 10$ mm) excluding muons and neutrinos and using the same jet reconstruction algorithms used for calorimeter jets. Similarly to the muon-in-jet correction at reconstruction level described in Section 4, particle-level muons are added to the particle-level jet if they are within $\Delta R = 0.2$ of a b -hadron. The

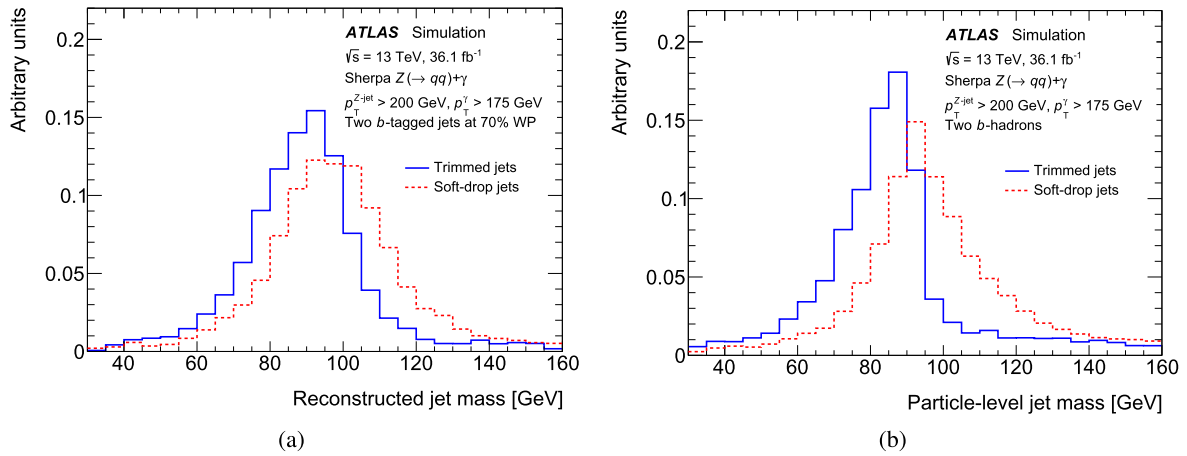


Fig. 1. Comparison of (a) the calibrated reconstructed Z-jet mass distribution and (b) the particle-level jet mass distribution of soft-drop (dashed line) and trimmed jets (solid line) in the signal region in the $Z\gamma$ sample.

mass of particle-level jets is defined as the invariant mass of the four-vector sum of its constituents. The jet mass distribution of soft-drop jets is significantly broader than that of trimmed jets for both the reconstructed jet mass, Fig. 1(a), and the particle-level jet mass, Fig. 1(b), whereas the distribution for trimmed jets is more asymmetric than for soft-drop jets at particle-level. This asymmetry is a feature of the trimming algorithm and is independent of the quark flavour from the Z boson decay. The jet mass is very stable with respect to pile-up for both jet definitions [53]. The soft-drop jets exhibit basically no pile-up dependence due to the constituent-level pile-up suppression techniques while the trimmed jet mass varies by 0.14 GeV per reconstructed vertex [53]. While Ref. [53] focusses on the hadronic decay of W bosons, it was found that the same conclusions hold as well for jets containing heavy flavour decays of Z bosons.

Track-jets Small-radius jets formed from charged-particle tracks are used as probes of b -hadrons associated with large- R jets that may contain the candidate $Z \rightarrow b\bar{b}$ jets. Track-jets are built with the anti- k_t algorithm with a radius parameter of $R = 0.2$ [12] from at least two 1D tracks with $p_T > 0.5$ GeV and $|\eta| < 2.5$ [54]. Only track-jets with $p_T > 10$ GeV and $|\eta| < 2.5$ are used and they are associated with the large- R calorimeter jets via ghost-association [51,55], in which the track-jets are included in the jet clustering procedure with infinitesimally small p_T such that they have no effect on the jet clustering result. Track-jets containing b -hadron decay products are tagged with a multivariate algorithm known as MV2c10, which exploits the presence of large-impact-parameter tracks, the topological decay chain reconstruction and the corresponding displaced vertices from b -hadron decays [56,57]. The MV2c10 algorithm is configured to achieve an efficiency of 70% for tagging b -jets in a MC sample of $t\bar{t}$ events, while rejecting 80% of c -jets and more than 99% of light (quark or gluon) jets in the same sample. This configuration is referred to as the 70% working point (WP). For MC samples, the tagging efficiencies are corrected to match those measured in data [54,58,59]. These small-radius track-jets are referred to as b -jets. By using this small- R definition, b -jets can be reliably identified in the dense environment of boosted bosons. Consequently, the number of associated b -jets ($N_{b\text{-jet}}$) provides an essential criterion for the identification of merged $Z \rightarrow b\bar{b}$ decays.

Photons Photon candidates are reconstructed from clusters of energy deposits in the EM calorimeter [60]. The photon energy is calibrated by applying the energy scales measured with $Z \rightarrow e^+e^-$ decays [61]. Identification requirements are applied to reduce the

contamination from π^0 or other neutral hadrons decaying into photons. Requirements on the shower shape in the EM calorimeter and on the energy fraction measured in the hadronic calorimeter are used to identify photons. Photons must satisfy the *tight* identification and isolation criteria defined in Ref. [60], and must have $|\eta| < 1.37$ or $1.52 < |\eta| < 2.37$. For MC samples, the photon reconstruction, identification and isolation efficiencies are corrected to match those measured in data [60,61]. The selected photon is required to have $p_T^\gamma > 175$ GeV, which is determined by an optimisation of the expected signal significance,² and to ensure that the trigger is fully efficient. The efficiency of the photon selection ranges between 95% and 98% for photons with $p_T^\gamma > 175$ GeV depending on the pseudorapidity of the photon. These selection criteria are inverted to form a sample of *non-tight* photons for the background estimate described in Section 5.

Quality requirements are applied to photon candidates to identify those arising from instrumental problems or non-collision background [62], and events containing such candidates are rejected. In addition, quality requirements are applied to remove events containing spurious jets from detector noise or out-of-time energy deposits in the calorimeter from cosmic rays or other non-collision sources [63].

Selected events are required to have at least one groomed large- R jet and at least one photon, with $\Delta R(\text{jet}, \gamma) > 1.0$ from the groomed large- R jet axis. The groomed large- R jet is required to have $p_T^{Z\text{-jet}} > 200$ GeV to capture both of the decay products of the $Z \rightarrow b\bar{b}$ decay, i.e. both jets from the b -quarks should be fully contained in the groomed large- R jet. In the signal region, the jets identified as candidate $Z \rightarrow b\bar{b}$ decays must contain at least two ghost-associated track-jets, and the two with the highest p_T must be tagged as b -jets ($N_{b\text{-jet}} = 2$).

5. Signal and background estimation

To extract the $Z(\rightarrow b\bar{b})\gamma$ signal from the data, signal and background templates obtained from MC simulation and from data are fitted to the observed $Z \rightarrow b\bar{b}$ candidate jet mass distribution using a binned maximum-likelihood fit. This procedure is repeated separately for each of the groomed jet definitions used to perform the measurement. The dominant background is γ + jets with gluon to $b\bar{b}$ splitting. Less significant background contributions are due to $t\bar{t} + \gamma$ and $W\gamma$ processes. Other backgrounds such as multijet and

² The expected signal significance is defined as $s/\sqrt{s+b}$, where s is the number of expected signal events and b is the number of expected background events.

Table 1

Definitions of the control regions (CR) and the signal region (SR) used for the data-driven background estimate of the γ + jets process.

	$N_{b\text{-jet}} = 0$	$N_{b\text{-jet}} = 1$	$N_{b\text{-jet}} = 2$
Non-tight γ	CR-A	CR-C	CR-E
Tight γ	CR-B	CR-D	SR

W/Z +jet processes, where a jet is misidentified as a photon, and the associated production of a Higgs boson with a γ are found to be negligible ($< 1\%$).

Templates of the jet mass distribution for the $Z(\rightarrow b\bar{b})\gamma$ signal, and for the $t\bar{t} + \gamma$ and $W\gamma$ backgrounds, are determined from MC simulation. In contrast, the template used to estimate the dominant background contribution from γ + jets processes is derived directly from the measured data without input from MC simulation. It is especially important to minimise the reliance on MC simulations for this process, as MC generators have not been tested thoroughly in the high p_T region of the $b\bar{b}$ production phase space for γ + jets.

The data-driven background estimate of the jet mass distribution for the γ + jets process relies on two features of the final state: the b -jet multiplicity (i.e. $N_{b\text{-jet}}$) and the photon identification criteria (i.e. tight vs non-tight). The b -jet multiplicity requirement is used to isolate the γ + jets process, which dominates in samples with $N_{b\text{-jet}} = 0$ or 1. Furthermore, the ratio of γ + jets yields ($N^{\gamma+\text{jets}}$) in events with tight compared with non-tight photons is observed to be approximately independent of $N_{b\text{-jet}}$. These two characteristics are used to model the expected γ + jets yield in the signal region via a transfer-factor (TF) method. This method extrapolates the signal region (SR) yield from control regions (CRs) with $N_{b\text{-jet}} = 1$ and the shape of the jet mass distribution in the signal region for the γ + jets background from CRs with $N_{b\text{-jet}} = 2$ but non-tight photons. The definitions of the different CRs are summarised in Table 1. In these CRs, the $t\bar{t} + \gamma$ and $W\gamma$ contributions are subtracted from the data, as the mass shape differs from that of γ + jets.

The γ + jets background estimates are constructed in 10 GeV bins of $Z \rightarrow b\bar{b}$ candidate jet mass. A bin size of 10 GeV is chosen based on the large- R jet mass resolution. For each jet mass bin, i , in each CR, the estimated yield of γ + jets events in that bin is calculated as:

$$N_{\text{CR},i}^{\gamma+\text{jets}} = N_{\text{CR},i} - N_{\text{CR},i}^{t\bar{t}+\gamma} - N_{\text{CR},i}^{W\gamma}$$

where $N_{\text{CR},i}^{t\bar{t}+\gamma}$ and $N_{\text{CR},i}^{W\gamma}$ are the number of $t\bar{t} + \gamma$ and $W\gamma$ events, respectively, taken directly from the MC simulation. The systematic uncertainties for $t\bar{t} + \gamma$ and $W\gamma$ contributions are described in Section 7. The contribution from signal events in each of these control regions is negligible compared to other processes and has no impact on the background estimation.

To obtain the estimate of the number of γ + jets events present in each bin of the jet mass distribution in the SR ($N_{\text{SR},i}^{\gamma+\text{jets}}$), the jet mass distribution from CR-E ($N_{\text{CR-E},i}^{\gamma+\text{jets}}$) is multiplied by a TF determined from the $N_{b\text{-jet}} = 1$ regions: CR-C and CR-D. This procedure may be summarised as

$$N_{\text{SR},i}^{\gamma+\text{jets}} = \left(\frac{N_{\text{CR-D},i}^{\gamma+\text{jets}}}{N_{\text{CR-C},i}^{\gamma+\text{jets}}} \right) N_{\text{CR-E},i}^{\gamma+\text{jets}},$$

where the ratio $N_{\text{CR-D},i}^{\gamma+\text{jets}}/N_{\text{CR-C},i}^{\gamma+\text{jets}}$ is the TF in each bin of the jet mass distribution. The value of the TF varies with jet mass, ranging from 1.2 for jet masses of 30 GeV to 0.8 at 160 GeV, and is within 5% of unity from 50 to 110 GeV. With this TF method, the

shape of the jet mass distribution in the signal region is determined from CR-E (with $N_{b\text{-jet}} = 2$) and the normalisation of each bin is determined from the $N_{b\text{-jet}} = 1$ control regions.

The validity of this approach relies on the assumption that the TF does not depend on $N_{b\text{-jet}}$. This is tested in data, using the $N_{b\text{-jet}} = 0$ sample as a cross-check, and in MC simulation using $N_{b\text{-jet}} = 0, 1$, and 2. The differences in the TFs between the $N_{b\text{-jet}} = 0$ and $N_{b\text{-jet}} = 1$ control regions in data are taken as systematic uncertainties in the TFs, as described in Section 7. The TF approach was further validated by comparing the TF, determined from the $N_{b\text{-jet}} = 1$ regions, in data and MC. Within their statistical precision, the TF were found to be compatible. Additionally, the reconstructed jet mass distribution of the data-driven background estimate in the SR is in good agreement with the jet mass distribution in γ + jets events simulated with SHERPA 2.1.1.

6. Definition of the observable and correction for detector effects

The reconstructed jet mass distributions from the signal regions are corrected to particle level in order to measure the full differential cross-section of the $Z \rightarrow b\bar{b}$ jet mass. Unfolding accounts for the effects of detector resolution and inefficiency and allows direct comparisons with particle-level predictions. The particle-level event selection is similar to the selection described in Section 4. Events are required to have at least one particle-level jet with $p_T > 200$ GeV, $|\eta| < 2.0$ and two ghost-associated b -hadrons. They are also required to have a particle-level photon with $p_T > 175$ GeV, $|\eta| < 1.37$ or $1.52 < |\eta| < 2.37$ and $\Delta R(\text{jet}, \gamma) > 1.0$.

The estimated background jet mass spectrum is subtracted from the data in the signal region, as discussed in Section 8. The background-subtracted distribution of the reconstructed jet mass is then unfolded using an iterative Bayesian technique [64] with one iteration. This technique is implemented in the RooUnfold framework [65]. One iteration is chosen to minimise the statistical uncertainties as well as the uncertainties associated with the unfolding method estimated with a data-driven closure test as described in Section 7. The unfolding procedure corrects for bin migrations between the particle-level and the reconstructed jet mass distribution using a response matrix that describes the probability for an event with a particle-level jet mass in bin i to be reconstructed in bin j . The response matrix is constructed from events that satisfy the event selection and fiducial region criteria at both the particle level and the reconstruction level. The particle-level jets and reconstructed jets are required to be matched within $\Delta R = 0.75$. Furthermore, the unfolding procedure corrects for events that satisfy either the particle-level or reconstructed selection criteria, but not both. The response matrix is obtained from the SHERPA $Z(\rightarrow b\bar{b})\gamma$ signal MC simulation. The $Z \rightarrow b\bar{b}$ candidate jet mass distribution was rebinned in the high jet mass region to improve the correlation between the reconstructed and particle-level jet mass. The unfolding results are found to be compatible when increasing the number of iterations used, at the expense of an increase in the statistical uncertainties. The unfolding procedure is also validated by unfolding the jet mass spectra using a singular value decomposition (SVD) technique [66] and within the statistical precision of the measurements, the results are found to be compatible.

7. Systematic uncertainties

Various sources of systematic uncertainties impact the $Z \rightarrow b\bar{b}$ candidate jet mass distribution. These are classified into experimental and theoretical uncertainties, and uncertainties related to the background estimate and the unfolding procedure. The systematic uncertainties can have an impact on the shape of the jet mass distribution and on the signal and background yields. Systematic

Table 2

The uncertainties in the integrated fiducial cross-section measurement from data in the signal region for trimmed and soft-drop jets. Multiple independent components are combined into groups of systematic uncertainties.

Source	Uncertainty [%]	
	Trimmed jets	Soft-drop jets
Luminosity	2.1	2.1
Jet energy resolution	0.4	< 0.1
Jet mass resolution	5.1	6.0
Jet energy and mass scale	7.2	7.4
b -tagging	5.3	5.8
Photon related	1.3	1.2
Muon related	0.1	< 0.1
Photon trigger	0.4	0.4
Transfer factor: 0-tag vs 1-tag	7.5	4.0
Transfer factor: statistical	2.9	1.5
$t\bar{t} + \gamma$ related	1.7	2.8
$W\gamma$ related	< 0.1	< 0.1
$Z\gamma$ modelling	12	15
Unfolding non-closure	9.4	5.8
Signal MC response: statistical	3.9	6.0
Background template: statistical	5.9	13
Fit statistical uncertainty	30	39
Total uncertainty	37	46

uncertainties are evaluated by varying each source by plus or minus one standard deviation of its uncertainty. The fit is repeated for each variation and the jet mass distribution unfolded to particle level. The jet energy and mass scale uncertainties are treated as correlated while all other sources of systematic uncertainties are treated as uncorrelated.

The impact of the systematic uncertainties on the integrated fiducial cross-section measurements, grouped by source, is summarised in Table 2.

For groomed large- R jets, the uncertainties in the energy and mass scales are estimated by using the double-ratio technique described in Ref. [44] by comparing the calorimeter jet properties with the measurements of the same jet reconstructed from tracks in the ID. The uncertainties in the jet mass and energy resolutions are assessed by applying additional smearing of the jet observables according to the uncertainty in their resolution measurements. An absolute uncertainty of 2% is used for the jet energy resolution while a relative uncertainty of 20% is used for the jet mass resolution, consistent with previous studies of both the trimmed and soft-drop jet definitions [20,67].

The b -tagging uncertainty is evaluated by varying the data-to-MC corrections in various kinematic regions, based on the measured tagging efficiency and mistag rates. These variations are applied separately to b -hadron jets, c -hadron jets, and light jets, leading to three uncorrelated systematic uncertainties. An additional uncertainty is included to account for the extrapolation to jets with p_T beyond the kinematic reach of the data calibration [54,58,59].

The impact of the systematic uncertainties on the photon reconstruction, identification and isolation efficiencies is studied by varying the scale factors, used to correct the respective efficiencies in simulation to match those observed in data, within their uncertainties. The uncertainties are determined from data samples of $Z \rightarrow \ell^+ \ell^- \gamma$ (with $\ell = e, \mu$), $Z \rightarrow e^+ e^-$, and inclusive photon events, using the methods described in Ref. [60]. Uncertainties in the photon energy scale and resolution are also taken into account [61].

The uncertainties associated with the muon momentum calibration and resolution, and the reconstruction and identification efficiency scale factors, are derived from $Z \rightarrow \mu^+ \mu^-$ events [52].

The uncertainty associated with the modelling of pile-up in the simulation is assessed by varying the reweighting of the pile-up in the simulation within its uncertainties. This uncertainty covers the

difference between the ratios of predicted and measured inelastic cross-section values [68].

The efficiency of the photon trigger is 100% for photons with $E_T^\gamma > 175$ GeV, with an uncertainty of 0.5% that is propagated through the unfolding.

The systematic uncertainties associated with the data-driven background template are estimated by deriving the bin-by-bin normalisation from CR-A and CR-B with $N_{b\text{-jet}} = 0$ instead of from the $N_{b\text{-jet}} = 1$ CRs as described in Section 5 (referred to as 'Transfer factor: 0-tag vs 1-tag'). An additional uncertainty in the bin-by-bin normalisation of the background template is derived by varying the jet mass distributions in CR-C and CR-D (with $N_{b\text{-jet}} = 1$) within their statistical uncertainty (referred to as 'Transfer factor: statistical').

The signal and background yields are estimated by performing a simultaneous fit to the data. The uncertainty in the normalisation of the background template, arising from the statistical uncertainty in the data, is referred to as the fit statistical uncertainty in the following.

The modelling uncertainties affecting the $W\gamma$ process are derived by comparing the nominal SHERPA 2.1.1 sample with one produced using the MADGRAPH [35] generator interfaced to PYTHIA 8. For the $t\bar{t} + \gamma$ background, three different sources of modelling uncertainties are considered: the uncertainty due to the parton shower and hadronisation is estimated by comparing the nominal samples produced using MADGRAPH interfaced to PYTHIA 8, with MADGRAPH interfaced to HERWIG 7 [69,70]; the uncertainty due to different initial- and final-state radiation conditions is estimated by using PYTHIA 8 tuned parameters with high or low QCD radiation activity; and the uncertainties due to the choice of renormalisation and factorisation scales are estimated by using alternative samples with the scales varied independently by factors of 2 and 0.5.

For the $Z\gamma$ process, the modelling uncertainty is derived by replacing the nominal sample with the alternative MADGRAPH sample, interfaced to PYTHIA 8. The fit is repeated with the alternative MC signal sample and then unfolded using the response matrix, signal efficiency and fake fraction from this alternative signal sample. Uncertainties in the signal efficiency and response matrix are already covered by experimental systematic errors outlined earlier.

The systematic uncertainty due to the dependence of the unfolding on the prior signal distribution, as obtained from MC simulations, is evaluated through a data-driven 'closure test'. The simulated signal sample is reweighted at particle level such that the distribution of the fully simulated reconstructed jet mass more closely matches the observed data. Pseudo-data from the reweighted signal MC sample are then unfolded using the response matrix from the original unweighted signal MC sample, and the unfolded result is compared with the reweighted particle-level distribution. Differences observed in this comparison are taken as systematic uncertainties in the unfolding, and are referred to as unfolding non-closure uncertainties in the following. The uncertainty due to the dependence on the number of unfolding iteration steps is negligible. The statistical uncertainties in the signal MC sample, used to build the response matrix, and background templates are also considered.

A bootstrapping procedure [71] is used to ensure that the systematic uncertainties are statistically significant. For each systematic uncertainty considered, pseudo-experiments are constructed from the data or MC simulation by assigning each event a weight taken from a Poisson distribution with unit mean. The statistical uncertainty in the systematic variation is taken as the RMS across the pseudo-experiments. The jet mass distribution for each of the systematic variations is then rebinned until a target significance of 1.5 standard deviations is achieved.

The dominant systematic uncertainties on the integrated fiducial cross-section measurements arise from the uncertainties in the

Table 3

The number of data events observed in the signal region, along with the composition of these events after the fit in the $30 < m^{Z\text{-jet}} < 160$ GeV mass range. Numbers are presented for trimmed and soft-drop jets at reconstruction level. Statistical and systematic uncertainties are added in quadrature. Systematic uncertainties are described in Section 7.

Process	Trimmed jets	Soft-drop jets
$Z\gamma$	215 ± 61	167 ± 73
$\gamma + \text{jets}$	4180 ± 90	4630 ± 100
$W\gamma$	39 ± 8	37 ± 8
$t\bar{t} + \gamma$	39 ± 12	40 ± 12
Total	4480 ± 110	4870 ± 120
Data	4475	4874

fit, the signal modelling, the data-driven background estimate, the jet mass and energy scales, and the jet mass resolution. The uncertainty in the pile-up modelling in MC simulation is found to be negligible.

As shown in Table 2 the impact of the statistical uncertainties on the fiducial cross-section of the response matrix and the background template is significantly different for trimmed and soft-drop jets. This behaviour can be explained by the differences of the signal and background jet mass distributions between trimmed and soft-drop jets and their interplay with the smoothing of those uncertainty components. For trimmed jets, only the variations in the core of the jet mass distributions are statistically significant while for soft-drop jets, the signal distribution is significantly wider and thus the tails also contribute to the systematic uncertainty. Furthermore, the background jet mass distribution of soft-drop jets is not as steeply falling as for trimmed jets. This results in less susceptibility to statistical fluctuations around the signal jet mass peak which would otherwise be reduced by the rebinning procedure introduced above.

8. Results

Results of the measurement of the jet mass distribution in $Z(\rightarrow b\bar{b})\gamma$ events are reported in the following three subsections; fit results and the calculation of the significance of the signal above the background, the unfolded fiducial cross-section measurement using the full measured jet mass spectrum, and the unfolded differential spectrum of the jet mass itself.

8.1. Fit results and significance estimate

The signal yield is extracted by simultaneously fitting the signal and the background templates described in Section 5 to the observed $Z \rightarrow b\bar{b}$ candidate jet mass ($m^{Z\text{-jet}}$) distribution. A binned maximum-likelihood fit is performed in the mass range between 30 and 160 GeV using a bin width of 10 GeV. The upper mass bound is chosen to exclude the mass region near the top quark mass while the lower mass bound is chosen to exclude the region of jet mass for which the uncertainty in the calibration is large and to protect against collinear singularities, as discussed in Section 4. The result of the fit to the reconstructed $Z \rightarrow b\bar{b}$ candidate jet mass distribution is shown in Figs. 2(a) and 2(b) for trimmed and soft-drop jets along with their corresponding background-subtracted data distributions in Figs. 2(c) and 2(d). The fitted signal yield is 215 ± 61 events for trimmed jets and 167 ± 73 events when using soft-drop jets as shown in Table 3.

The 13 bins of the $Z \rightarrow b\bar{b}$ candidate jet mass distribution are combined in a profile likelihood fit [72] to extract the expected and observed significances. Systematic uncertainties are included in the

Table 4

Expected and observed significance values (in numbers of standard deviations) for trimmed and soft-drop jets for a mass range between 30 and 160 GeV.

	Trimmed jets	Soft-drop jets
Expected significance	3.8	2.7
Observed significance	3.9	2.7

fit as nuisance parameters and are assumed to be Gaussian distributed. The expected and observed significances of the Standard Model prediction fitted to the observed data for the $Z(\rightarrow b\bar{b})\gamma$ production are summarised in Table 4. For each jet definition, the observed significance is consistent with the expectation. Differences in the significance between the two jet definitions are related to the differences in both the jet mass resolution and the fiducial cross-sections between trimmed and soft-drop jets, which affect the signal and background yields in the 30–160 GeV mass window.

8.2. Integrated fiducial cross-section measurement

The measured integrated fiducial cross-sections in the boosted (high p_T) $Z \rightarrow b\bar{b}$ region are listed in Table 5. The integrated fiducial cross-section is extracted from the ratio of the unfolded yield of signal events and the total integrated luminosity. The measurements are compared with the SHERPA 2.1.1 and MADGRAPH+PYTHIA 8 LO predictions described in Section 3. MADGRAPH+PYTHIA 8 predicts around 30% fewer events than the samples generated with SHERPA. Within the current uncertainties on the measurement, both predictions are consistent with the measured cross-sections for soft-drop jets. For trimmed jets, larger differences can be observed between the MADGRAPH+PYTHIA 8 prediction and the measured cross-section. The uncertainties in the measured integrated fiducial cross-section results are summarised in Table 2. The dominant source of systematic uncertainty is the fit uncertainty for both jet definitions. The uncertainty in the normalisation of the background template has a large impact on the cross-section measurement because of the order of magnitude difference between the estimated numbers of signal and background events.

8.3. Differential fiducial cross-section measurement

The differential fiducial cross-section of $Z(\rightarrow b\bar{b})\gamma$ production as a function of the $Z \rightarrow b\bar{b}$ jet mass, obtained from the unfolded data in the signal region, is shown in Fig. 3 for trimmed and soft-drop jets. As a comparison, the prediction from SHERPA 2.1.1 at LO is also shown. Statistical uncertainties are significant for the differential fiducial cross-section measurement in the tails of the jet mass distribution.

9. Conclusion

The fully unfolded differential jet mass spectrum for the high- p_T $Z \rightarrow b\bar{b}$ signal using the $Z\gamma$ final state and the fiducial production cross-section are measured in 36.1 fb^{-1} of pp collisions at $\sqrt{s} = 13$ TeV recorded in 2015 and 2016 by the ATLAS detector. The high- p_T $Z \rightarrow b\bar{b}$ signal is reconstructed using large- R jets and jet substructure techniques, including double subjet b -tagging. Two different grooming algorithms are used in this analysis: trimming and soft drop. These grooming algorithms exhibit differences in the measured shapes of the jet mass spectra and the resulting precision of those measurements. The soft drop jet mass spectrum is observed to be broader and more symmetric than that of trimmed jets. The precision of the fiducial cross-section measured is slightly

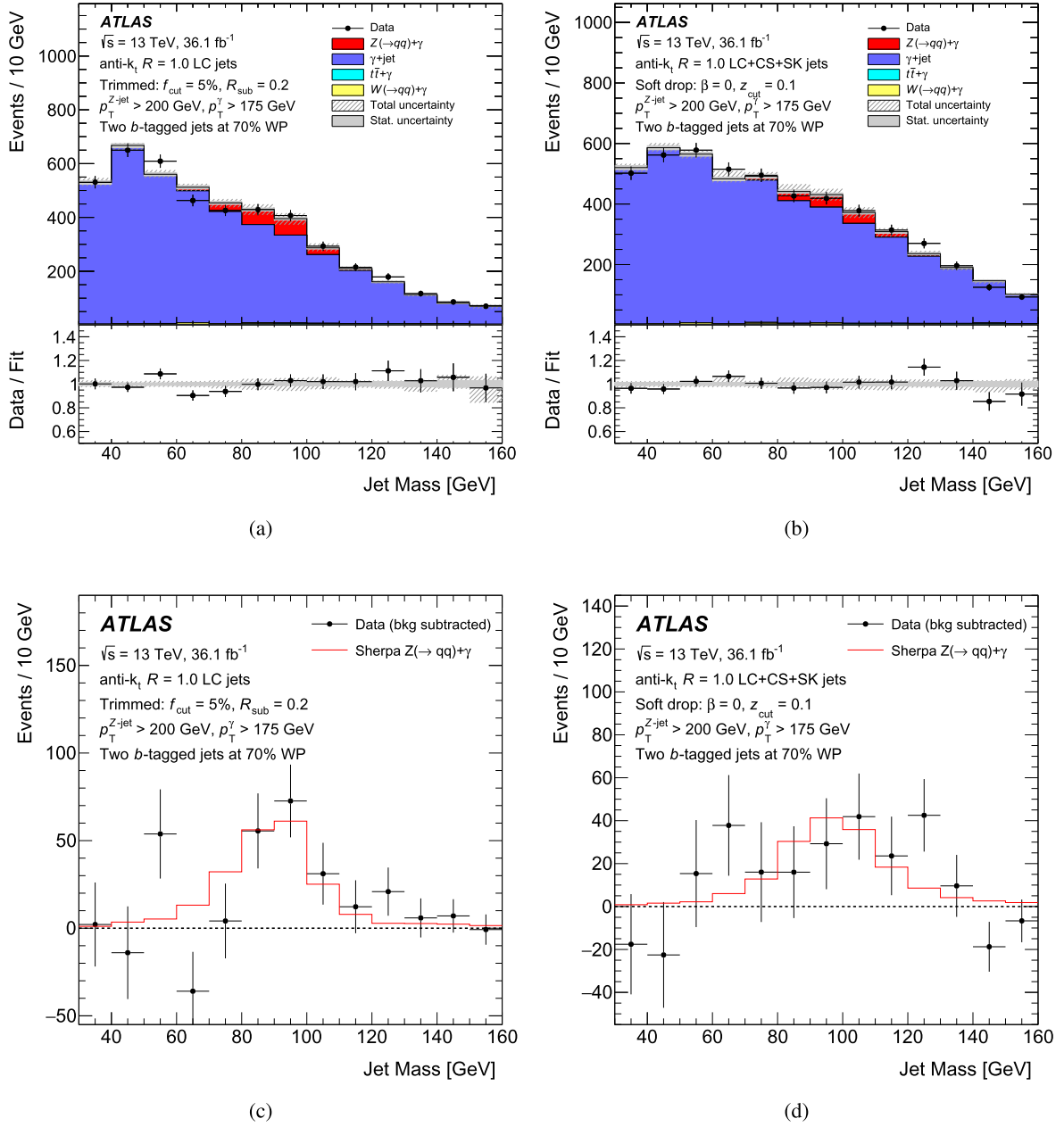


Fig. 2. The reconstructed jet mass distribution in the signal region (a, b) after fitting the SHERPA 2.1.1 signal model and background templates to the data and (c, d) the corresponding background-subtracted distributions for (a, c) trimmed and (b, d) soft-drop jets. The ratio of data to the fitted signal plus background is shown at the bottom in Figures (a) and (b). The background-subtracted jet mass distributions in data are compared with the reconstructed signal jet mass distributions in the nominal Monte Carlo simulation. The error bars on the background-subtracted data distribution are statistical only. The SHERPA signal model and background template are scaled to fit the data as described in Section 5.

Table 5

Measured and predicted cross-section for $Z(\rightarrow b\bar{b})\gamma$ in the $p_T^{Z\text{-jet}} > 200$ GeV, $30 < m^{Z\text{-jet}} < 160$ GeV and $p_T^\gamma > 175$ GeV region.

Jet definition		$\sigma(Z(\rightarrow b\bar{b})\gamma, p_T^{Z\text{-jet}} > 200$ GeV, $p_T^\gamma > 175$ GeV, $30 < m^{Z\text{-jet}} < 160$ GeV) [fb]
Trimmed jets	Data	17.0 ± 5.0 (stat.) ± 3.6 (syst.)
	SHERPA $Z\gamma$ prediction	13.4 ± 0.2 (stat.)
	MADGRAPH+PYTHIA 8 $Z\gamma$ prediction	9.1 ± 0.1 (stat.)
Soft-drop jets	Data	12.5 ± 4.9 (stat.) ± 3.1 (syst.)
	SHERPA $Z\gamma$ prediction	15.4 ± 0.1 (stat.)
	MADGRAPH+PYTHIA 8 $Z\gamma$ prediction	10.2 ± 0.1 (stat.)

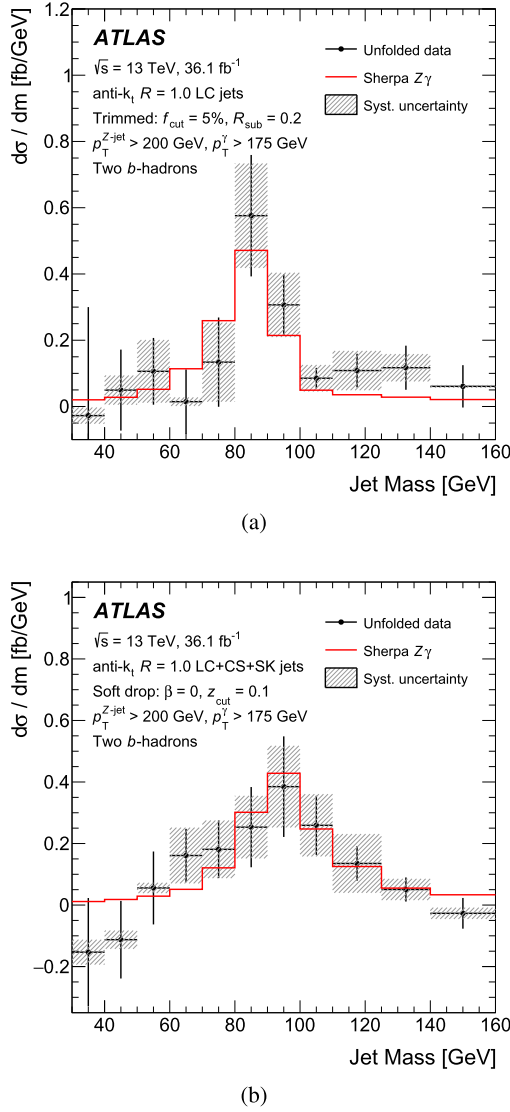


Fig. 3. Unfolded distribution of the $Z \rightarrow b\bar{b}$ candidate jet mass from background-subtracted data in the signal region along with the predictions from SHERPA 2.1.1. Results for (a) trimmed and (b) soft-drop jets are shown. The error bars correspond to the statistical uncertainty while the hatched band corresponds to the total systematic uncertainty in the measurement. The statistical uncertainty in the SHERPA signal is negligible and not shown in the figure.

better for trimmed jets. Within the fiducial regions defined for each jet definition as $p_T^{Z\text{-jet}} > 200$ GeV, $30 < m^{Z\text{-jet}} < 160$ GeV and $p_T^\gamma > 175$ GeV, the production cross-sections are measured to be:

$$\sigma_{Z(\rightarrow b\bar{b})\gamma}^{\text{trimming}} = 17.0 \pm 5.0 \text{ (stat.)} \pm 3.6 \text{ (syst.) fb,}$$

$$\sigma_{Z(\rightarrow b\bar{b})\gamma}^{\text{soft drop}} = 12.5 \pm 4.9 \text{ (stat.)} \pm 3.1 \text{ (syst.) fb.}$$

The integrated fiducial cross-section measurements and the differential cross-section of the jet mass of the boosted $Z \rightarrow b\bar{b}$ decay are found to be in agreement with the LO predictions from SHERPA and MADGRAPH+PYTHIA 8 (integrated), and from SHERPA (differential), respectively, within the current statistical and systematic uncertainties. Future measurements of resonant $b\bar{b}$ decays will need to account for the observed experimental features of these different grooming algorithms in concert with the availability of precision theoretical calculations of the jet mass spectra, or lack thereof.

Declaration of competing interest

The authors declare that they have no known competing financial interests or personal relationships that could have appeared to influence the work reported in this paper.

Acknowledgements

We thank CERN for the very successful operation of the LHC, as well as the support staff from our institutions without whom ATLAS could not be operated efficiently.

We acknowledge the support of ANPCyT, Argentina; YerPhI, Armenia; ARC, Australia; BMWFW and FWF, Austria; ANAS, Azerbaijan; SSTC, Belarus; CNPq and FAPESP, Brazil; NSERC, NRC and CFI, Canada; CERN; ANID, Chile; CAS, MOST and NSFC, China; COLCIENCIAS, Colombia; MSMT CR, MPO CR and VSC CR, Czech Republic; DNRF and DNSRC, Denmark; IN2P3-CNRS and CEA-DRF/IRFU, France; SRNSFG, Georgia; BMBF, HGF and MPG, Germany; GSRT, Greece; RGC and Hong Kong SAR, China; ISF and Benozziyo Center, Israel; INFN, Italy; MEXT and JSPS, Japan; CNRST, Morocco; NWO, Netherlands; RCN, Norway; MNiSW and NCN, Poland; FCT, Portugal; MNE/IFA, Romania; JINR; MES of Russia and NRC KI, Russian Federation; MESTD, Serbia; MSSR, Slovakia; ARRS and MIZŠ, Slovenia; DST/NRF, South Africa; MICINN, Spain; SRC and Wallenberg Foundation, Sweden; SERI, SNSF and Cantons of Bern and Geneva, Switzerland; MOST, Taiwan; TAEK, Turkey; STFC, United Kingdom; DOE and NSF, United States of America. In addition, individual groups and members have received support from BCKDF, Canarie, Compute Canada, CRC and IVADO, Canada; Beijing Municipal Science & Technology Commission, China; COST, ERC, ERDF, Horizon 2020 and Marie Skłodowska-Curie Actions, European Union; Investissements d'Avenir Labex, Investissements d'Avenir IDEX and ANR, France; DFG and AvH Foundation, Germany; Herakleitos, Thales and Aristeia programmes co-financed by EU-ESF and the Greek NSRF, Greece; BSF-NSF and GIF, Israel; La Caixa Banking Foundation, CERCA Programme Generalitat de Catalunya and PROMETEO and GenT Programmes Generalitat Valenciana, Spain; Göran Gustafssons Stiftelse, Sweden; The Royal Society and Leverhulme Trust, United Kingdom.

The crucial computing support from all WLCG partners is acknowledged gratefully, in particular from CERN, the ATLAS Tier-1 facilities at TRIUMF (Canada), NDGF (Denmark, Norway, Sweden), CC-IN2P3 (France), KIT/GridKA (Germany), INFN-CNAF (Italy), NL-T1 (Netherlands), PIC (Spain), ASGC (Taiwan), RAL (UK) and BNL (USA), the Tier-2 facilities worldwide and large non-WLCG resource providers. Major contributors of computing resources are listed in Ref. [73].

References

- [1] ATLAS Collaboration, The ATLAS experiment at the CERN Large Hadron Collider, *J. Instrum.* 3 (2008) S08003.
- [2] ATLAS Collaboration, Properties of $g \rightarrow b\bar{b}$ at small opening angles in pp collisions with the ATLAS detector at $\sqrt{s} = 13$ TeV, *Phys. Rev. D* 99 (2019) 052004, arXiv:1812.09283 [hep-ex].
- [3] ATLAS Collaboration, Search for heavy resonances decaying into a W or Z boson and a Higgs boson in final states with leptons and b -jets in 36 fb^{-1} of $\sqrt{s} = 13$ TeV pp collisions with the ATLAS detector, *J. High Energy Phys.* 03 (2018) 174, arXiv:1712.06518 [hep-ex].
- [4] ATLAS Collaboration, Search for heavy resonances decaying to a photon and a hadronically decaying $Z/W/H$ boson in pp collisions at $\sqrt{s} = 13$ TeV with the ATLAS detector, *Phys. Rev. D* 98 (2018) 032015, arXiv:1805.01908 [hep-ex].
- [5] ATLAS Collaboration, Measurement of the cross section of high transverse momentum $Z \rightarrow b\bar{b}$ production in proton-proton collisions at $\sqrt{s} = 8$ TeV with the ATLAS detector, *Phys. Lett. B* 738 (2014) 25, arXiv:1404.7042 [hep-ex].
- [6] CMS Collaboration, Inclusive search for a highly boosted Higgs boson decaying to a bottom quark-antiquark pair, *Phys. Rev. Lett.* 120 (2018) 071802, arXiv:1709.05543 [hep-ex].

- [7] ATLAS Collaboration, Identification of boosted Higgs bosons decaying into b -quark pairs with the ATLAS detector at 13 TeV, arXiv:1906.11005 [hep-ex], 2019.
- [8] M. Cacciari, G.P. Salam, G. Soyez, The anti- k_t jet clustering algorithm, *J. High Energy Phys.* 04 (2008) 063, arXiv:0802.1189 [hep-ph].
- [9] ATLAS Collaboration, Performance of jet substructure techniques for large- R jets in proton–proton collisions at $\sqrt{s} = 7$ TeV using the ATLAS detector, *J. High Energy Phys.* 09 (2013) 076, arXiv:1306.4945 [hep-ex].
- [10] D. Krohn, J. Thaler, L.-T. Wang, Jet trimming, *J. High Energy Phys.* 02 (2010) 084, arXiv:0912.1342 [hep-ph].
- [11] A.J. Larkoski, S. Marzani, G. Soyez, J. Thaler, Soft drop, *J. High Energy Phys.* 05 (2014) 146, arXiv:1402.2657 [hep-ph].
- [12] ATLAS Collaboration, Flavor tagging with track-jets in boosted topologies with the ATLAS detector, ATL-PHYS-PUB-2014-013, <https://cds.cern.ch/record/1750681>, 2014.
- [13] M. Dasgupta, A. Fregoso, S. Marzani, G.P. Salam, Towards an understanding of jet substructure, *J. High Energy Phys.* 09 (2013) 029, arXiv:1307.0007 [hep-ph].
- [14] ATLAS Collaboration, Identification of boosted, hadronically decaying W bosons and comparisons with ATLAS data taken at $\sqrt{s} = 8$ TeV, *Eur. Phys. J. C* 76 (2016) 154, arXiv:1510.05821 [hep-ex].
- [15] S. Marzani, L. Schunk, G. Soyez, A study of jet mass distributions with grooming, *J. High Energy Phys.* 07 (2017) 132, arXiv:1704.02210 [hep-ph].
- [16] Z.-B. Kang, K. Lee, X. Liu, F. Ringer, The groomed and ungroomed jet mass distribution for inclusive jet production at the LHC, *J. High Energy Phys.* 10 (2018) 137, arXiv:1803.03645 [hep-ph].
- [17] C. Frye, A.J. Larkoski, M.D. Schwartz, K. Yan, Precision physics with pile-up insensitive observables, arXiv:1603.06375 [hep-ph], 2016.
- [18] C. Frye, A.J. Larkoski, M.D. Schwartz, K. Yan, Factorization for groomed jet substructure beyond the next-to-leading logarithm, *J. High Energy Phys.* 07 (2016) 064, arXiv:1603.09338 [hep-ph].
- [19] T. Becher, M.D. Schwartz, A precise determination of α_s from LEP thrust data using effective field theory, *J. High Energy Phys.* 07 (2008) 034, arXiv:0803.0342 [hep-ph].
- [20] ATLAS Collaboration, Measurement of the soft-drop jet mass in pp collisions at $\sqrt{s} = 13$ TeV with the ATLAS detector, *Phys. Rev. Lett.* 121 (2018) 092001, arXiv:1711.08341 [hep-ex].
- [21] CMS Collaboration, Measurements of the differential jet cross section as a function of the jet mass in dijet events from proton–proton collisions at $\sqrt{s} = 13$ TeV, *J. High Energy Phys.* 11 (2018) 113, arXiv:1807.05974 [hep-ex].
- [22] CMS Collaboration, Studies of jet mass in dijet and W/Z +jet events, *J. High Energy Phys.* 05 (2013) 090, arXiv:1303.4811 [hep-ex].
- [23] ATLAS Collaboration, ATLAS insertable b-layer technical design report, ATLAS-TDR-19, <https://cds.cern.ch/record/1291633>, 2010; ATLAS insertable B-layer technical design report addendum, ATLAS-TDR-19-ADD-1, <https://cds.cern.ch/record/1451888>, 2012.
- [24] B. Abbott, et al., Production and integration of the ATLAS insertable b-layer, *J. Instrum.* 13 (2018) T05008, arXiv:1803.00844 [physics.ins-det].
- [25] ATLAS Collaboration, Performance of the ATLAS trigger system in 2015, *Eur. Phys. J. C* 77 (2017) 317, arXiv:1611.09661 [hep-ex].
- [26] ATLAS Collaboration, Luminosity determination in pp collisions at $\sqrt{s} = 13$ TeV using the ATLAS detector at the LHC, ATLAS-CONF-2019-021, <http://cdsweb.cern.ch/record/2677054>, 2019.
- [27] G. Avoni, et al., The new LUCID-2 detector for luminosity measurement and monitoring in ATLAS, *J. Instrum.* 13 (2018) P07017.
- [28] ATLAS Collaboration, The ATLAS simulation infrastructure, *Eur. Phys. J. C* 70 (2010) 823, arXiv:1005.4568 [physics.ins-det].
- [29] S. Agostinelli, et al., GEANT4: a simulation toolkit, *Nucl. Instrum. Methods A* 506 (2003) 250.
- [30] T. Sjöstrand, S. Mrenna, P.Z. Skands, A brief introduction to PYTHIA 8.1, *Comput. Phys. Commun.* 178 (2008) 852, arXiv:0710.3820 [hep-ph].
- [31] ATLAS Collaboration, Summary of ATLAS Pythia 8 tunes, ATL-PHYS-PUB-2012-003, <https://cds.cern.ch/record/1474107>, 2012.
- [32] R.D. Ball, et al., Parton distributions with LHC data, *Nucl. Phys. B* 867 (2013) 244–289, arXiv:1207.1303 [hep-ph].
- [33] T. Gleisberg, et al., Event generation with SHERPA 1.1, *J. High Energy Phys.* 02 (2009) 007, arXiv:0811.4622 [hep-ph].
- [34] H.-L. Lai, et al., New parton distributions for collider physics, *Phys. Rev. D* 82 (2010) 074024, arXiv:1007.2241 [hep-ph].
- [35] J. Alwall, et al., The automated computation of tree-level and next-to-leading order differential cross sections, and their matching to parton shower simulations, *J. High Energy Phys.* 07 (2014) 079, arXiv:1405.0301 [hep-ph].
- [36] ATLAS Collaboration, ATLAS Pythia 8 tunes to 7 TeV data, ATL-PHYS-PUB-2014-021, <https://cds.cern.ch/record/1966419>, 2014.
- [37] ATLAS Collaboration, Measurements of inclusive and differential fiducial cross-sections of $t\bar{t}\gamma$ production in leptonic final states at $\sqrt{s} = 13$ TeV in ATLAS, *Eur. Phys. J. C* 79 (2019) 382, arXiv:1812.01697 [hep-ex].
- [38] ATLAS Collaboration, Vertex reconstruction performance of the ATLAS detector at $\sqrt{s} = 13$ TeV, ATL-PHYS-PUB-2015-026, <https://cds.cern.ch/record/2037717>, 2015.
- [39] ATLAS Collaboration, Topological cell clustering in the ATLAS calorimeters and its performance in LHC Run 1, *Eur. Phys. J. C* 77 (2017) 490, arXiv:1603.02934 [hep-ex].
- [40] M. Cacciari, G.P. Salam, Dispelling the N^3 myth for the k_t jet-finder, *Phys. Lett. B* 641 (2006) 57, arXiv:hep-ph/0512210 [hep-ph].
- [41] M. Cacciari, G.P. Salam, G. Soyez, FastJet user manual, *Eur. Phys. J. C* 72 (2012) 1896, arXiv:1111.6097 [hep-ph].
- [42] S. Catani, Y.L. Dokshitzer, M.H. Seymour, B.R. Webber, Longitudinally invariant k_t clustering algorithms for hadron hadron collisions, *Nucl. Phys. B* 406 (1993) 187.
- [43] S.D. Ellis, D.E. Soper, Successive combination jet algorithm for hadron collisions, *Phys. Rev. D* 48 (1993) 3160, arXiv:hep-ph/9305266 [hep-ph].
- [44] ATLAS Collaboration, In situ calibration of large- R jet energy and mass in 13 TeV proton–proton collisions with the ATLAS detector, *Eur. Phys. J. C* 79 (2019) 135, arXiv:1807.09477 [hep-ex].
- [45] Y.L. Dokshitzer, G.D. Leder, S. Moretti, B.R. Webber, Better jet clustering algorithms, *J. High Energy Phys.* 08 (1997) 001, arXiv:hep-ph/9707323 [hep-ph].
- [46] M. Wobisch, T. Wengler, Hadronization corrections to jet cross-sections in deep inelastic scattering, in: Monte Carlo Generators for HERA Physics, Proceedings, Workshop, Hamburg, Germany, 1998–1999, 1998, p. 270, arXiv:hep-ph/9907280 [hep-ph].
- [47] ATLAS Collaboration, Impact of alternative inputs and grooming methods on large- R jet reconstruction in ATLAS, ATL-PHYS-PUB-2017-020, <https://cds.cern.ch/record/2297485>, 2017.
- [48] M. Cacciari, G.P. Salam, G. Soyez, SoftKiller, a particle-level pileup removal method, *Eur. Phys. J. C* 75 (2015) 59, arXiv:1407.0408 [hep-ph].
- [49] P. Berta, M. Spousta, D.W. Miller, R. Leitner, Particle-level pileup subtraction for jets and jet shapes, *J. High Energy Phys.* 06 (2014) 092, arXiv:1403.3108 [hep-ex].
- [50] ATLAS Collaboration, Constituent-level pile-up mitigation techniques in ATLAS, ATLAS-CONF-2017-065, <https://cds.cern.ch/record/2281055>, 2017.
- [51] M. Cacciari, G.P. Salam, Pileup subtraction using jet areas, *Phys. Lett. B* 659 (2008) 119, arXiv:0707.1378 [hep-ph].
- [52] ATLAS Collaboration, Muon reconstruction performance of the ATLAS detector in proton–proton collision data at $\sqrt{s} = 13$ TeV, *Eur. Phys. J. C* 76 (2016) 292, arXiv:1603.05598 [hep-ex].
- [53] ATLAS Collaboration, Optimisation of large-radius jet reconstruction for the ATLAS detector in 13 TeV proton–proton collisions, arXiv:2009.04986 [hep-ex], 2020.
- [54] ATLAS Collaboration, Measurements of b -jet tagging efficiency with the ATLAS detector using $t\bar{t}$ events at $\sqrt{s} = 13$ TeV, *J. High Energy Phys.* 08 (2018) 089, arXiv:1805.01845 [hep-ex].
- [55] M. Cacciari, G.P. Salam, G. Soyez, The catchment area of jets, *J. High Energy Phys.* 04 (2008) 005, arXiv:0802.1188 [hep-ph].
- [56] ATLAS Collaboration, Performance of b -jet identification in the ATLAS experiment, *J. Instrum.* 11 (2016) P04008, arXiv:1512.01094 [hep-ex].
- [57] ATLAS Collaboration, Optimisation of the ATLAS b -tagging performance for the 2016 LHC run, ATL-PHYS-PUB-2016-012, <https://cds.cern.ch/record/2160731>, 2016.
- [58] ATLAS Collaboration, Calibration of light-flavour b -jet mistagging rates using ATLAS proton–proton collision data at $\sqrt{s} = 13$ TeV, ATLAS-CONF-2018-006, <https://cds.cern.ch/record/2314418>, 2018.
- [59] ATLAS Collaboration, Measurement of b -tagging efficiency of c -jets in $t\bar{t}$ events using a likelihood approach with the ATLAS detector, ATLAS-CONF-2018-001, <https://cds.cern.ch/record/2306649>, 2018.
- [60] ATLAS Collaboration, Measurement of the photon identification efficiencies with the ATLAS detector using LHC Run 2 data collected in 2015 and 2016, *Eur. Phys. J. C* 79 (2019) 205, arXiv:1810.05087 [hep-ex].
- [61] ATLAS Collaboration, Electron and photon energy calibration with the ATLAS detector using 2015–2016 LHC proton–proton collision data, *J. Instrum.* 14 (2019) P03017, arXiv:1812.03848 [hep-ex].
- [62] ATLAS Collaboration, Monitoring and data quality assessment of the ATLAS liquid argon calorimeter, *J. Instrum.* 9 (2014) P07024, arXiv:1405.3768 [hep-ex].
- [63] ATLAS Collaboration, Selection of jets produced in 13 TeV proton–proton collisions with the ATLAS detector, ATLAS-CONF-2015-029, <https://cds.cern.ch/record/2037702>, 2015.
- [64] G. D’Agostini, Improved iterative Bayesian unfolding, arXiv:1010.0632 [physics.data-an], 2010.
- [65] T. Auye, Unfolding algorithms and tests using RooUnfold, arXiv:1105.1160 [physics.data-an], 2011.
- [66] A. Hocker, V. Kartvelishvili, SVD approach to data unfolding, *Nucl. Instrum. Methods A* 372 (1996) 469, arXiv:hep-ph/9509307 [hep-ph].
- [67] ATLAS Collaboration, Jet mass and substructure of inclusive jets in $\sqrt{s} = 7$ TeV pp collisions with the ATLAS experiment, *J. High Energy Phys.* 05 (2012) 128, arXiv:1203.4606 [hep-ex].
- [68] ATLAS Collaboration, Measurement of the inelastic proton–proton cross section at $\sqrt{s} = 13$ TeV with the ATLAS detector at the LHC, *Phys. Rev. Lett.* 117 (2016) 182002, arXiv:1606.02625 [hep-ex].

- [69] M. Bahr, et al., Herwig++ physics and manual, *Eur. Phys. J. C* 58 (2008) 639, arXiv:0803.0883 [hep-ph].
- [70] J. Bellm, et al., Herwig 7.0/Herwig++ 3.0 release note, *Eur. Phys. J. C* 76 (2016) 196, arXiv:1512.01178 [hep-ph].
- [71] G. Bohm, G. Zech, *Introduction to Statistics and Data Analysis for Physicists*, Verlag Deutsches Elektronen-Synchrotron, ISBN 978-3-935702-41-6, 2010.
- [72] K. Cranmer, G. Lewis, L. Moneta, A. Shibata, W. Verkerke, HistFactory: a tool for creating statistical models for use with RooFit and RooStats, tech. rep. CERN-OPEN-2012-016, New York U., 2012, <https://cds.cern.ch/record/1456844>.
- [73] ATLAS Collaboration, ATLAS computing acknowledgements, ATL-SOFT-PUB-2020-001, <https://cds.cern.ch/record/2717821>.

The ATLAS Collaboration

G. Aad¹⁰², B. Abbott¹²⁹, D.C. Abbott¹⁰³, O. Abdinov^{13,*}, A. Abed Abud^{71a,71b}, K. Abeling⁵³, D.K. Abhayasinghe⁹⁴, S.H. Abidi¹⁶⁸, O.S. AbouZeid⁴⁰, N.L. Abraham¹⁵⁷, H. Abramowicz¹⁶², H. Abreu¹⁶¹, Y. Abulaiti⁶, B.S. Acharya^{67a,67b,q}, B. Achkar⁵³, S. Adachi¹⁶⁴, L. Adam¹⁰⁰, C. Adam Bourdarios⁶⁵, L. Adamczyk^{84a}, L. Adamek¹⁶⁸, J. Adelman¹²¹, M. Adersberger¹¹⁴, A. Adiguzel^{12c,an}, S. Adorni⁵⁴, T. Adye¹⁴⁴, A.A. Affolder¹⁴⁶, Y. Afik¹⁶¹, C. Agapopoulou⁶⁵, M.N. Agaras³⁸, A. Aggarwal¹¹⁹, C. Agheorghiesei^{27c}, J.A. Aguilar-Saavedra^{140f,140a,am}, F. Ahmadov⁸⁰, W.S. Ahmed¹⁰⁴, X. Ai^{15a}, G. Aielli^{74a,74b}, S. Akatsuka⁸⁶, T.P.A. Åkesson⁹⁷, E. Akilli⁵⁴, A.V. Akimov¹¹¹, K. Al Khoury⁶⁵, G.L. Alberghi^{23b,23a}, J. Albert¹⁷⁷, M.J. Alconada Verzini¹⁶², S. Alderweireldt³⁶, M. Aleksa³⁶, I.N. Aleksandrov⁸⁰, C. Alexa^{27b}, D. Alexandre¹⁹, T. Alexopoulos¹⁰, A. Alfonsi¹²⁰, M. Alhroob¹²⁹, B. Ali¹⁴², G. Alimonti^{69a}, J. Alison³⁷, S.P. Alkire¹⁴⁹, C. Allaire⁶⁵, B.M.M. Allbrooke¹⁵⁷, B.W. Allen¹³², P.P. Allport²¹, A. Aloisio^{70a,70b}, A. Alonso⁴⁰, F. Alonso⁸⁹, C. Alpigiani¹⁴⁹, A.A. Alshehri⁵⁷, M. Alvarez Estevez⁹⁹, D. Álvarez Piqueras¹⁷⁵, M.G. Alvigi^{70a,70b}, Y. Amaral Coutinho^{81b}, A. Ambler¹⁰⁴, L. Ambroz¹³⁵, C. Amelung²⁶, D. Amidei¹⁰⁶, S.P. Amor Dos Santos^{140a}, S. Amoroso⁴⁶, C.S. Amrouche⁵⁴, F. An⁷⁹, C. Anastopoulos¹⁵⁰, N. Andari¹⁴⁵, T. Andeen¹¹, C.F. Anders^{61b}, J.K. Anders²⁰, A. Andreazza^{69a,69b}, V. Andrei^{61a}, C.R. Anelli¹⁷⁷, S. Angelidakis³⁸, A. Angerami³⁹, A.V. Anisenkov^{122b,122a}, A. Annovi^{72a}, C. Antel^{61a}, M.T. Anthony¹⁵⁰, M. Antonelli⁵¹, D.J.A. Antrim¹⁷², F. Anulli^{73a}, M. Aoki⁸², J.A. Aparisi Pozo¹⁷⁵, L. Aperio Bella³⁶, G. Arabidze¹⁰⁷, J.P. Araque^{140a}, V. Araujo Ferraz^{81b}, R. Araujo Pereira^{81b}, C. Arcangeletti⁵¹, A.T.H. Arce⁴⁹, F.A. Arduh⁸⁹, J-F. Arguin¹¹⁰, S. Argyropoulos⁷⁸, J.-H. Arling⁴⁶, A.J. Armbruster³⁶, L.J. Armitage⁹³, A. Armstrong¹⁷², O. Arnaez¹⁶⁸, H. Arnold¹²⁰, A. Artamonov^{124,*}, G. Artoni¹³⁵, S. Artz¹⁰⁰, S. Asai¹⁶⁴, N. Asbah⁵⁹, E.M. Asimakopoulou¹⁷³, L. Asquith¹⁵⁷, K. Assamagan²⁹, R. Astalos^{28a}, R.J. Atkin^{33a}, M. Atkinson¹⁷⁴, N.B. Atlay¹⁵², H. Atmani⁶⁵, K. Augsten¹⁴², G. Avolio³⁶, R. Avramidou^{60a}, M.K. Ayoub^{15a}, A.M. Azoulay^{169b}, G. Azuelos^{110,ba}, M.J. Baca²¹, H. Bachacou¹⁴⁵, K. Bachas^{68a,68b}, M. Backes¹³⁵, F. Backman^{45a,45b}, P. Bagnaia^{73a,73b}, M. Bahmani⁸⁵, H. Bahrasemani¹⁵³, A.J. Bailey¹⁷⁵, V.R. Bailey¹⁷⁴, J.T. Baines¹⁴⁴, M. Bajic⁴⁰, C. Bakalis¹⁰, O.K. Baker¹⁸⁴, P.J. Bakker¹²⁰, D. Bakshi Gupta⁸, S. Balaji¹⁵⁸, E.M. Baldin^{122b,122a}, P. Balek¹⁸¹, F. Balli¹⁴⁵, W.K. Balunas¹³⁵, J. Balz¹⁰⁰, E. Banas⁸⁵, A. Bandyopadhyay²⁴, Sw. Banerjee^{182,k}, A.A.E. Bannoura¹⁸³, L. Barak¹⁶², W.M. Barbe³⁸, E.L. Barberio¹⁰⁵, D. Barberis^{55b,55a}, M. Barbero¹⁰², T. Barillari¹¹⁵, M-S. Barisits³⁶, J. Barkeloo¹³², T. Barklow¹⁵⁴, R. Barnea¹⁶¹, S.L. Barnes^{60c}, B.M. Barnett¹⁴⁴, R.M. Barnett¹⁸, Z. Barnovska-Blenessy^{60a}, A. Baroncelli^{60a}, G. Barone²⁹, A.J. Barr¹³⁵, L. Barranco Navarro^{45a,45b}, F. Barreiro⁹⁹, J. Barreiro Guimarães da Costa^{15a}, S. Barsov¹³⁸, R. Bartoldus¹⁵⁴, G. Bartolini¹⁰², A.E. Barton⁹⁰, P. Bartos^{28a}, A. Basalae⁴⁶, A. Bassalat^{65,au}, R.L. Bates⁵⁷, S.J. Batista¹⁶⁸, S. Batlamous^{35e}, J.R. Batley³², B. Batool¹⁵², M. Battaglia¹⁴⁶, M. Bauce^{73a,73b}, F. Bauer¹⁴⁵, K.T. Bauer¹⁷², H.S. Bawa^{31,o}, J.B. Beacham⁴⁹, T. Beau¹³⁶, P.H. Beauchemin¹⁷¹, F. Becherer⁵², P. Bechtel²⁴, H.C. Beck⁵³, H.P. Beck^{20,u}, K. Becker⁵², M. Becker¹⁰⁰, C. Becot⁴⁶, A. Beddall^{12d}, A.J. Beddall^{12a}, V.A. Bednyakov⁸⁰, M. Bedognetti¹²⁰, C.P. Bee¹⁵⁶, T.A. Beermann⁷⁷, M. Begalli^{81b}, M. Begel²⁹, A. Behara¹⁵⁶, J.K. Behr⁴⁶, F. Beisiegel²⁴, A.S. Bell⁹⁵, G. Bella¹⁶², L. Bellagamba^{23b}, A. Bellerive³⁴, P. Bellos⁹, K. Beloborodov^{122b,122a}, K. Belotskiy¹¹², N.L. Belyaev¹¹², D. Bencheekroun^{35a}, N. Benekos¹⁰, Y. Benhammou¹⁶², D.P. Benjamin⁶, M. Benoit⁵⁴, J.R. Bensinger²⁶, S. Bentvelsen¹²⁰, L. Beresford¹³⁵, M. Beretta⁵¹, D. Berge⁴⁶, E. Bergeaas Kuutmann¹⁷³, N. Berger⁵, B. Bergmann¹⁴², L.J. Bergsten²⁶, J. Beringer¹⁸, S. Berlendis⁷, N.R. Bernard¹⁰³, G. Bernardi¹³⁶, C. Bernius¹⁵⁴, F.U. Bernlochner²⁴, T. Berry⁹⁴, P. Berta¹⁰⁰, C. Bertella^{15a}, I.A. Bertram⁹⁰, G.J. Besjes⁴⁰, O. Bessidskaia Bylund¹⁸³, N. Besson¹⁴⁵, A. Bethani¹⁰¹, S. Bethke¹¹⁵, A. Betti²⁴, A.J. Bevan⁹³, J. Beyer¹¹⁵, R. Bi¹³⁹, R.M. Bianchi¹³⁹, O. Biebel¹¹⁴, D. Biedermann¹⁹, R. Bielski³⁶, K. Bierwagen¹⁰⁰, N.V. Biesuz^{72a,72b}, M. Biglietti^{75a}, T.R.V. Billoud¹¹⁰, M. Bindi⁵³, A. Bingul^{12d}, C. Bini^{73a,73b}, S. Biondi^{23b,23a}, M. Birman¹⁸¹, T. Bisanz⁵³, J.P. Biswal¹⁶², A. Bitadze¹⁰¹, C. Bittrich⁴⁸, K. Bjørke¹³⁴, K.M. Black²⁵, T. Blazek^{28a}, I. Bloch⁴⁶, C. Blocker²⁶, A. Blue⁵⁷, U. Blumenschein⁹³, G.J. Bobbink¹²⁰, V.S. Bobrovnikov^{122b,122a}, S.S. Bocchetta⁹⁷, A. Bocci⁴⁹, D. Bogavac¹⁴, A.G. Bogdanchikov^{122b,122a}, C. Bohm^{45a}, V. Boisvert⁹⁴, P. Bokan⁵³, T. Bold^{84a},

A.S. Boldyrev¹¹³, A.E. Bolz^{61b}, M. Bomben¹³⁶, M. Bona⁹³, J.S. Bonilla¹³², M. Boonekamp¹⁴⁵,
 H.M. Borecka-Bielska⁹¹, A. Borisov¹²³, G. Borissov⁹⁰, J. Bortfeldt³⁶, D. Bortoletto¹³⁵, V. Bortolotto^{74a,74b},
 D. Boscherini^{23b}, M. Bosman¹⁴, J.D. Bossio Sola¹⁰⁴, K. Bouaouda^{35a}, J. Boudreau¹³⁹,
 E.V. Bouhova-Thacker⁹⁰, D. Boumediene³⁸, S.K. Boutle⁵⁷, A. Boveia¹²⁷, J. Boyd³⁶, D. Boye^{33c,av},
 I.R. Boyko⁸⁰, A.J. Bozson⁹⁴, J. Bracinik²¹, N. Brahimi¹⁰², G. Brandt¹⁸³, O. Brandt^{61a}, F. Braren⁴⁶,
 B. Brau¹⁰³, J.E. Brau¹³², W.D. Breaden Madden⁵⁷, K. Brendlinger⁴⁶, L. Brenner⁴⁶, R. Brenner¹⁷³,
 S. Bressler¹⁸¹, B. Brickwedde¹⁰⁰, D.L. Briglin²¹, D. Britton⁵⁷, D. Britzger¹¹⁵, I. Brock²⁴, R. Brock¹⁰⁷,
 G. Brooijmans³⁹, W.K. Brooks^{147d}, E. Brost¹²¹, J.H. Broughton²¹, P.A. Bruckman de Renstrom⁸⁵,
 D. Bruncko^{28b}, A. Bruni^{23b}, G. Bruni^{23b}, L.S. Bruni¹²⁰, S. Bruno^{74a,74b}, B.H. Brunt³², M. Bruschi^{23b},
 N. Bruscino¹³⁹, P. Bryant³⁷, L. Bryngemark⁹⁷, T. Buanes¹⁷, Q. Buat³⁶, P. Buchholz¹⁵², A.G. Buckley⁵⁷,
 I.A. Budagov⁸⁰, M.K. Bugge¹³⁴, F. Bühner⁵², O. Bulekov¹¹², T.J. Burch¹²¹, S. Burdin⁹¹, C.D. Burgard¹²⁰,
 A.M. Burger¹³⁰, B. Burghgrave⁸, J.T.P. Burr⁴⁶, J.C. Burzynski¹⁰³, V. Büscher¹⁰⁰, E. Buschmann⁵³,
 P.J. Bussey⁵⁷, J.M. Butler²⁵, C.M. Buttar⁵⁷, J.M. Butterworth⁹⁵, P. Butti³⁶, W. Buttinger³⁶, A. Buzatu¹⁵⁹,
 A.R. Buzykaev^{122b,122a}, G. Cabras^{23b,23a}, S. Cabrera Urbán¹⁷⁵, D. Caforio⁵⁶, H. Cai¹⁷⁴, V.M.M. Cairo¹⁵⁴,
 O. Cakir^{4a}, N. Calace³⁶, P. Calafiura¹⁸, A. Calandri¹⁰², G. Calderini¹³⁶, P. Calfayan⁶⁶, G. Callea⁵⁷,
 L.P. Caloba^{81b}, S. Calvente Lopez⁹⁹, D. Calvet³⁸, S. Calvet³⁸, T.P. Calvet¹⁵⁶, M. Calvetti^{72a,72b},
 R. Camacho Toro¹³⁶, S. Camarda³⁶, D. Camarero Munoz⁹⁹, P. Camarri^{74a,74b}, D. Cameron¹³⁴,
 R. Caminal Armadans¹⁰³, C. Camincher³⁶, S. Campana³⁶, M. Campanelli⁹⁵, A. Camplani⁴⁰,
 A. Campoverde¹⁵², V. Canale^{70a,70b}, A. Canesse¹⁰⁴, M. Cano Bret^{60c}, J. Cantero¹³⁰, T. Cao¹⁶², Y. Cao¹⁷⁴,
 M.D.M. Capeans Garrido³⁶, M. Capua^{41b,41a}, R. Cardarelli^{74a}, F. Cardillo¹⁵⁰, G. Carducci^{41b,41a},
 I. Carli¹⁴³, T. Carli³⁶, G. Carlino^{70a}, B.T. Carlson¹³⁹, L. Carminati^{69a,69b}, R.M.D. Carney^{45a,45b},
 S. Caron¹¹⁹, E. Carquin^{147d}, S. Carrá⁴⁶, J.W.S. Carter¹⁶⁸, M.P. Casado^{14,f}, A.F. Casha¹⁶⁸, D.W. Casper¹⁷²,
 R. Castelijin¹²⁰, F.L. Castillo¹⁷⁵, V. Castillo Gimenez¹⁷⁵, N.F. Castro^{140a,140e}, A. Catinaccio³⁶,
 J.R. Catmore¹³⁴, A. Cattai³⁶, J. Caudron²⁴, V. Cavaliere²⁹, E. Cavallaro¹⁴, M. Cavalli-Sforza¹⁴,
 V. Cavasinni^{72a,72b}, E. Celebi^{12b}, F. Ceradini^{75a,75b}, L. Cerda Alberich¹⁷⁵, K. Cerny¹³¹, A.S. Cerqueira^{81a},
 A. Cerri¹⁵⁷, L. Cerrito^{74a,74b}, F. Cerutti¹⁸, A. Cervelli^{23b,23a}, S.A. Cetin^{12b}, D. Chakraborty¹²¹,
 S.K. Chan⁵⁹, W.S. Chan¹²⁰, W.Y. Chan⁹¹, J.D. Chapman³², B. Chargeishvili^{160b}, D.G. Charlton²¹,
 T.P. Charman⁹³, C.C. Chau³⁴, S. Che¹²⁷, A. Chegwidden¹⁰⁷, S. Chekanov⁶, S.V. Chekulaev^{169a},
 G.A. Chelkov^{80,as}, M.A. Chelstowska³⁶, B. Chen⁷⁹, C. Chen^{60a}, C.H. Chen⁷⁹, H. Chen²⁹, J. Chen^{60a},
 J. Chen³⁹, S. Chen¹³⁷, S.J. Chen^{15c}, X. Chen^{15b,az}, Y. Chen⁸³, Y-H. Chen⁴⁶, H.C. Cheng^{63a}, H.J. Cheng^{15a},
 A. Cheplakov⁸⁰, E. Cheremushkina¹²³, R. Cherkaoui El Moursli^{35e}, E. Cheu⁷, K. Cheung⁶⁴,
 T.J.A. Chevalérias¹⁴⁵, L. Chevalier¹⁴⁵, V. Chiarella⁵¹, G. Chiarelli^{72a}, G. Chiodini^{68a}, A.S. Chisholm^{36,21},
 A. Chitan^{27b}, I. Chiu¹⁶⁴, Y.H. Chiu¹⁷⁷, M.V. Chizhov⁸⁰, K. Choi⁶⁶, A.R. Chomont^{73a,73b}, S. Chouridou¹⁶³,
 Y.S. Chow¹²⁰, M.C. Chu^{63a}, X. Chu^{15a,15d}, J. Chudoba¹⁴¹, A.J. Chuinard¹⁰⁴, J.J. Chwastowski⁸⁵,
 L. Chytka¹³¹, K.M. Ciesla⁸⁵, D. Cinca⁴⁷, V. Cindro⁹², I.A. Cioară^{27b}, A. Ciocio¹⁸, F. Ciroto^{70a,70b},
 Z.H. Citron^{181,m}, M. Citterio^{69a}, D.A. Ciubotaru^{27b}, B.M. Ciungu¹⁶⁸, A. Clark⁵⁴, M.R. Clark³⁹, P.J. Clark⁵⁰,
 C. Clement^{45a,45b}, Y. Coadou¹⁰², M. Cokal^{67a,67c}, A. Coccaro^{55b}, J. Cochran⁷⁹, H. Cohen¹⁶²,
 A.E.C. Coimbra³⁶, L. Colasurdo¹¹⁹, B. Cole³⁹, A.P. Colijn¹²⁰, J. Collot⁵⁸, P. Conde Muiño^{140a,g},
 E. Coniavitis⁵², S.H. Connell^{33c}, I.A. Connelly⁵⁷, S. Constantinescu^{27b}, F. Conventi^{70a,bb},
 A.M. Cooper-Sarkar¹³⁵, F. Cormier¹⁷⁶, K.J.R. Cormier¹⁶⁸, L.D. Corpe⁹⁵, M. Corradi^{73a,73b}, E.E. Corrigan⁹⁷,
 F. Corriveau^{104,ai}, M.J. Costa¹⁷⁵, F. Costanza⁵, D. Costanzo¹⁵⁰, G. Cowan⁹⁴, J.W. Cowley³², J. Crane¹⁰¹,
 K. Cranmer¹²⁵, S.J. Crawley⁵⁷, R.A. Creager¹³⁷, S. Crépé-Renaudin⁵⁸, F. Crescioli¹³⁶, M. Cristinziani²⁴,
 V. Croft¹²⁰, G. Crosetti^{41b,41a}, A. Cueto⁵, T. Cuhadar Donszelmann¹⁵⁰, A.R. Cukierman¹⁵⁴,
 S. Czekaierda⁸⁵, P. Czodrowski³⁶, M.J. Da Cunha Sargedas De Sousa^{60b}, J.V. Da Fonseca Pinto^{81b},
 C. Da Via¹⁰¹, W. Dabrowski^{84a}, T. Dado^{28a}, S. Dahbi^{35e}, T. Dai¹⁰⁶, C. Dallapiccola¹⁰³, M. Dam⁴⁰,
 G. D'amen^{23b,23a}, V. D'Amico^{75a,75b}, J. Damp¹⁰⁰, J.R. Dandoy¹³⁷, M.F. Daneri³⁰, N.P. Dang^{182,k},
 N.S. Dann¹⁰¹, M. Danninger¹⁷⁶, V. Dao³⁶, G. Darbo^{55b}, O. Dartsis⁵, A. Dattagupta¹³², T. Daubney⁴⁶,
 S. D'Auria^{69a,69b}, W. Davey²⁴, C. David⁴⁶, T. Davidek¹⁴³, D.R. Davis⁴⁹, I. Dawson¹⁵⁰, K. De⁸,
 R. De Asmundis^{70a}, M. De Beurs¹²⁰, S. De Castro^{23b,23a}, S. De Cecco^{73a,73b}, N. De Groot¹¹⁹,
 P. de Jong¹²⁰, H. De la Torre¹⁰⁷, A. De Maria^{15c}, D. De Pedis^{73a}, A. De Salvo^{73a}, U. De Sanctis^{74a,74b},
 M. De Santis^{74a,74b}, A. De Santo¹⁵⁷, K. De Vasconcelos Corga¹⁰², J.B. De Vivie De Regie⁶⁵,
 C. Debenedetti¹⁴⁶, D.V. Dedovich⁸⁰, A.M. Deiana⁴², M. Del Gaudio^{41b,41a}, J. Del Peso⁹⁹,
 Y. Delabat Diaz⁴⁶, D. Delgove⁶⁵, F. Deliot^{145,t}, C.M. Delitzsch⁷, M. Della Pietra^{70a,70b}, D. Della Volpe⁵⁴,

A. Dell'Acqua³⁶, L. Dell'Asta^{74a,74b}, M. Delmastro⁵, C. Delporte⁶⁵, P.A. Delsart⁵⁸, D.A. DeMarco¹⁶⁸, S. Demers¹⁸⁴, M. Demichev⁸⁰, G. Demontigny¹¹⁰, S.P. Denisov¹²³, D. Denysiuk¹²⁰, L. D'Eramo¹³⁶, D. Derendarz⁸⁵, J.E. Derkaoui^{35d}, F. Derue¹³⁶, P. Dervan⁹¹, K. Desch²⁴, C. Deterre⁴⁶, K. Dette¹⁶⁸, C. Deutsch²⁴, M.R. Devesa³⁰, P.O. Deviveiros³⁶, A. Dewhurst¹⁴⁴, S. Dhaliwal²⁶, F.A. Di Bello⁵⁴, A. Di Ciaccio^{74a,74b}, L. Di Ciaccio⁵, W.K. Di Clemente¹³⁷, C. Di Donato^{70a,70b}, A. Di Girolamo³⁶, G. Di Gregorio^{72a,72b}, B. Di Micco^{75a,75b}, R. Di Nardo¹⁰³, K.F. Di Petrillo⁵⁹, R. Di Sipio¹⁶⁸, D. Di Valentino³⁴, C. Diaconu¹⁰², F.A. Dias⁴⁰, T. Dias Do Vale^{140a}, M.A. Diaz^{147a}, J. Dickinson¹⁸, E.B. Diehl¹⁰⁶, J. Dietrich¹⁹, S. Díez Cornell⁴⁶, A. Dimitrievska¹⁸, W. Ding^{15b}, J. Dingfelder²⁴, F. Dittus³⁶, F. Djama¹⁰², T. Djobava^{160b}, J.I. Djuvsland¹⁷, M.A.B. Do Vale¹⁴⁸, M. Dobre^{27b}, D. Dodsworth²⁶, C. Doglioni⁹⁷, J. Dolejsi¹⁴³, Z. Dolezal¹⁴³, M. Donadelli^{81c}, B. Dong^{60c}, J. Donini³⁸, A. D'onofrio⁹³, M. D'Onofrio⁹¹, J. Dopke¹⁴⁴, A. Doria^{70a}, M.T. Dova⁸⁹, A.T. Doyle⁵⁷, E. Drechsler¹⁵³, E. Dreyer¹⁵³, T. Dreyer⁵³, A.S. Drobac¹⁷¹, Y. Duan^{60b}, F. Dubinin¹¹¹, M. Dubovsky^{28a}, A. Dubreuil⁵⁴, E. Duchovni¹⁸¹, G. Duckeck¹¹⁴, A. Ducourthial¹³⁶, O.A. Ducu¹¹⁰, D. Duda¹¹⁵, A. Dudarev³⁶, A.C. Dudder¹⁰⁰, E.M. Duffield¹⁸, L. Dufлот⁶⁵, M. Dührssen³⁶, C. Dülsen¹⁸³, M. Dumancic¹⁸¹, A.E. Dumitriu^{27b}, A.K. Duncan⁵⁷, M. Dunford^{61a}, A. Duperrin¹⁰², H. Duran Yildiz^{4a}, M. Düren⁵⁶, A. Durglishvili^{160b}, D. Duschinger⁴⁸, B. Dutta⁴⁶, D. Duvnjak¹, G.I. Dyckes¹³⁷, M. Dyndal³⁶, S. Dysch¹⁰¹, B.S. Dziedzic⁸⁵, K.M. Ecker¹¹⁵, R.C. Edgar¹⁰⁶, T. Eifert³⁶, G. Eigen¹⁷, K. Einsweiler¹⁸, T. Ekelof¹⁷³, H. El Jarrari^{35e}, M. El Kacimi^{35c}, R. El Kosseifi¹⁰², V. Ellajosyula¹⁷³, M. Ellert¹⁷³, F. Ellinghaus¹⁸³, A.A. Elliot⁹³, N. Ellis³⁶, J. Elmsheuser²⁹, M. Elsing³⁶, D. Emelianov¹⁴⁴, A. Emerman³⁹, Y. Enari¹⁶⁴, J.S. Ennis¹⁷⁹, M.B. Epland⁴⁹, J. Erdmann⁴⁷, A. Ereditato²⁰, M. Errenst³⁶, M. Escalier⁶⁵, C. Escobar¹⁷⁵, O. Estrada Pastor¹⁷⁵, E. Etzion¹⁶², H. Evans⁶⁶, A. Ezhilov¹³⁸, F. Fabbri⁵⁷, L. Fabbri^{23b,23a}, V. Fabiani¹¹⁹, G. Facini⁹⁵, R.M. Faisca Rodrigues Pereira^{140a}, R.M. Fakhruddinov¹²³, S. Falciano^{73a}, P.J. Falke⁵, S. Falke⁵, J. Faltova¹⁴³, Y. Fang^{15a}, Y. Fang^{15a}, G. Fanourakis⁴⁴, M. Fanti^{69a,69b}, M. Faraj^{67a,67c,w}, A. Farbin⁸, A. Farilla^{75a}, E.M. Farina^{71a,71b}, T. Farooque¹⁰⁷, S. Farrell¹⁸, S.M. Farrington⁵⁰, P. Farthouat³⁶, F. Fassi^{35e}, P. Fassnacht³⁶, D. Fassouliotis⁹, M. Fauci Giannelli⁵⁰, W.J. Fawcett³², L. Fayard⁶⁵, O.L. Fedin^{138,r}, W. Fedorko¹⁷⁶, M. Feickert⁴², S. Feigl¹³⁴, L. Feligioni¹⁰², A. Fell¹⁵⁰, C. Feng^{60b}, E.J. Feng³⁶, M. Feng⁴⁹, M.J. Fenton⁵⁷, A.B. Fenyuk¹²³, J. Ferrando⁴⁶, A. Ferrante¹⁷⁴, A. Ferrari¹⁷³, P. Ferrari¹²⁰, R. Ferrari^{71a}, D.E. Ferreira de Lima^{61b}, A. Ferrer¹⁷⁵, D. Ferrere⁵⁴, C. Ferretti¹⁰⁶, F. Fiedler¹⁰⁰, A. Filipčič⁹², F. Filthaut¹¹⁹, K.D. Finelli²⁵, M.C.N. Fiolhais^{140a,140c,a}, L. Fiorini¹⁷⁵, F. Fischer¹¹⁴, W.C. Fisher¹⁰⁷, I. Fleck¹⁵², P. Fleischmann¹⁰⁶, R.R.M. Fletcher¹³⁷, T. Flick¹⁸³, B.M. Flierl¹¹⁴, L. Flores¹³⁷, L.R. Flores Castillo^{63a}, F.M. Follega^{76a,76b}, N. Fomin¹⁷, J.H. Foo¹⁶⁸, G.T. Forcolin^{76a,76b}, A. Formica¹⁴⁵, F.A. Förster¹⁴, A.C. Forti¹⁰¹, A.G. Foster²¹, M.G. Foti¹³⁵, D. Fournier⁶⁵, H. Fox⁹⁰, P. Francavilla^{72a,72b}, S. Francescato^{73a,73b}, M. Franchini^{23b,23a}, S. Franchino^{61a}, D. Francis³⁶, L. Franconi²⁰, M. Franklin⁵⁹, A.N. Fray⁹³, B. Freund¹¹⁰, W.S. Freund^{81b}, E.M. Freundlich⁴⁷, D.C. Frizzell¹²⁹, D. Froidevaux³⁶, J.A. Frost¹³⁵, C. Fukunaga¹⁶⁵, E. Fullana Torregrosa¹⁷⁵, E. Fumagalli^{55b,55a}, T. Fusayasu¹¹⁶, J. Fuster¹⁷⁵, A. Gabrielli^{23b,23a}, A. Gabrielli¹⁸, G.P. Gach^{84a}, S. Gadatsch⁵⁴, P. Gadow¹¹⁵, G. Gagliardi^{55b,55a}, L.G. Gagnon¹¹⁰, C. Galea^{27b}, B. Galhardo^{140a}, G.E. Gallardo¹³⁵, E.J. Gallas¹³⁵, B.J. Gallop¹⁴⁴, P. Gallus¹⁴², G. Galster⁴⁰, R. Gamboa Goni⁹³, K.K. Gan¹²⁷, S. Ganguly¹⁸¹, J. Gao^{60a}, Y. Gao⁹¹, Y.S. Gao^{31,o}, C. García¹⁷⁵, J.E. García Navarro¹⁷⁵, J.A. García Pascual^{15a}, C. Garcia-Argos⁵², M. Garcia-Sciveres¹⁸, R.W. Gardner³⁷, N. Garelli¹⁵⁴, S. Gargiulo⁵², V. Garonne¹³⁴, A. Gaudiello^{55b,55a}, G. Gaudio^{71a}, I.L. Gavrilenko¹¹¹, A. Gavrilyuk¹²⁴, C. Gay¹⁷⁶, G. Gaycken²⁴, E.N. Gazis¹⁰, A.A. Geanta^{27b}, C.N.P. Gee¹⁴⁴, J. Geisen⁵³, M. Geisen¹⁰⁰, M.P. Geisler^{61a}, C. Gemme^{55b}, M.H. Genest⁵⁸, C. Geng¹⁰⁶, S. Gentile^{73a,73b}, S. George⁹⁴, T. Gerialis⁴⁴, L.O. Gerlach⁵³, P. Gessinger-Befurt¹⁰⁰, G. Gessner⁴⁷, S. Ghasemi¹⁵², M. Ghasemi Bostanabad¹⁷⁷, A. Ghosh⁶⁵, A. Ghosh⁷⁸, B. Giacobbe^{23b}, S. Giagu^{73a,73b}, N. Giangiacomi^{23b,23a}, P. Giannetti^{72a}, A. Giannini^{70a,70b}, S.M. Gibson⁹⁴, M. Gignac¹⁴⁶, D. Gillberg³⁴, G. Gilles¹⁸³, D.M. Gingrich^{3,ba}, M.P. Giordani^{67a,67c}, F.M. Giorgi^{23b}, P.F. Giraud¹⁴⁵, G. Giugliarelli^{67a,67c}, D. Giugni^{69a}, F. Giuli^{74a,74b}, S. Gkaitatzis¹⁶³, I. Gkialas^{9,i}, E.L. Gkoukousis¹⁴, P. Gkoutoumis¹⁰, L.K. Gladilin¹¹³, C. Glasman⁹⁹, J. Glatzer¹⁴, P.C.F. Glaysher⁴⁶, A. Glazov⁴⁶, M. Goblirsch-Kolb²⁶, S. Goldfarb¹⁰⁵, T. Golling⁵⁴, D. Golubkov¹²³, A. Gomes^{140a,140b}, R. Goncalves Gama⁵³, R. Gonçalves^{140a}, G. Gonella⁵², L. Gonella²¹, A. Gongadze⁸⁰, F. Gonnella²¹, J.L. Gonski⁵⁹, S. González de la Hoz¹⁷⁵, S. Gonzalez-Sevilla⁵⁴, G.R. Gonzalvo Rodriguez¹⁷⁵, L. Goossens³⁶, P.A. Gorbounov¹²⁴, H.A. Gordon²⁹, B. Gorini³⁶, E. Gorini^{68a,68b}, A. Gorišek⁹², A.T. Goshaw⁴⁹, M.I. Gostkin⁸⁰, C.A. Gottardo²⁴, M. Gouighri^{35b}, D. Goujdami^{35c}, A.G. Goussiou¹⁴⁹, N. Govender^{33c,b}, C. Goy⁵, E. Gozani¹⁶¹,

I. Grabowska-Bold^{84a}, E.C. Graham⁹¹, J. Gramling¹⁷², E. Gramstad¹³⁴, S. Grancagnolo¹⁹, M. Grandi¹⁵⁷, V. Gratchev¹³⁸, P.M. Gravila^{27f}, F.G. Gravili^{68a,68b}, C. Gray⁵⁷, H.M. Gray¹⁸, C. Grefe²⁴, K. Gregersen⁹⁷, I.M. Gregor⁴⁶, P. Grenier¹⁵⁴, K. Grevtsov⁴⁶, C. Grieco¹⁴, N.A. Grieser¹²⁹, J. Griffiths⁸, A.A. Grillo¹⁴⁶, K. Grimm^{31,n}, S. Grinstein^{14,ac}, J.-F. Grivaz⁶⁵, S. Groh¹⁰⁰, E. Gross¹⁸¹, J. Grosse-Knetter⁵³, Z.J. Grout⁹⁵, C. Grud¹⁰⁶, A. Grummer¹¹⁸, L. Guan¹⁰⁶, W. Guan¹⁸², J. Guenther³⁶, A. Guerguichon⁶⁵, J.G.R. Guerrero Rojas¹⁷⁵, F. Guescini¹¹⁵, D. Guest¹⁷², R. Gugel⁵², T. Guillemin⁵, S. Guindon³⁶, U. Gul⁵⁷, J. Guo^{60c}, W. Guo¹⁰⁶, Y. Guo^{60a,v}, Z. Guo¹⁰², R. Gupta⁴⁶, S. Gurbuz^{12c}, G. Gustavino¹²⁹, P. Gutierrez¹²⁹, C. Gutsche⁹⁵, C. Guyot¹⁴⁵, M.P. Guzik^{84a}, C. Gwenlan¹³⁵, C.B. Gwilliam⁹¹, A. Haas¹²⁵, C. Haber¹⁸, H.K. Hadavand⁸, N. Haddad^{35e}, A. Hadeef^{60a}, S. Hageböck³⁶, M. Hagihara¹⁷⁰, M. Haleem¹⁷⁸, J. Haley¹³⁰, G. Halladjian¹⁰⁷, G.D. Hallowell¹⁰², K. Hamacher¹⁸³, P. Hamal¹³¹, K. Hamano¹⁷⁷, H. Hamdaoui^{35e}, G.N. Hamity¹⁵⁰, K. Han^{60a,ab}, L. Han^{60a}, S. Han^{15a}, K. Hanagaki^{82,z}, M. Hance¹⁴⁶, D.M. Handl¹¹⁴, B. Haney¹³⁷, R. Hankache¹³⁶, E. Hansen⁹⁷, J.B. Hansen⁴⁰, J.D. Hansen⁴⁰, M.C. Hansen²⁴, P.H. Hansen⁴⁰, E.C. Hanson¹⁰¹, K. Hara¹⁷⁰, A.S. Hard¹⁸², T. Harenberg¹⁸³, S. Harkusha¹⁰⁸, P.F. Harrison¹⁷⁹, N.M. Hartmann¹¹⁴, Y. Hasegawa¹⁵¹, A. Hasib⁵⁰, S. Hassani¹⁴⁵, S. Haug²⁰, R. Hauser¹⁰⁷, L.B. Havener³⁹, M. Havranek¹⁴², C.M. Hawkes²¹, R.J. Hawkins³⁶, D. Hayden¹⁰⁷, C. Hayes¹⁵⁶, R.L. Hayes¹⁷⁶, C.P. Hays¹³⁵, J.M. Hays⁹³, H.S. Hayward⁹¹, S.J. Haywood¹⁴⁴, F. He^{60a}, M.P. Heath⁵⁰, V. Hedberg⁹⁷, L. Heelan⁸, S. Heer²⁴, K.K. Heidegger⁵², W.D. Heidorn⁷⁹, J. Heilman³⁴, S. Heim⁴⁶, T. Heim¹⁸, B. Heinemann^{46,aw}, J.J. Heinrich¹³², L. Heinrich³⁶, C. Heinz⁵⁶, J. Hejbal¹⁴¹, L. Helary^{61b}, A. Held¹⁷⁶, S. Hellesund¹³⁴, C.M. Helling¹⁴⁶, S. Hellman^{45a,45b}, C. Helsens³⁶, R.C.W. Henderson⁹⁰, Y. Heng¹⁸², S. Henkelmann¹⁷⁶, A.M. Henriques Correia³⁶, G.H. Herbert¹⁹, H. Herde²⁶, V. Herget¹⁷⁸, Y. Hernández Jiménez^{33e}, H. Herr¹⁰⁰, M.G. Herrmann¹¹⁴, T. Herrmann⁴⁸, G. Herten⁵², R. Hertenberger¹¹⁴, L. Hervas³⁶, T.C. Herwig¹³⁷, G.G. Hesketh⁹⁵, N.P. Hessey^{169a}, A. Higashida¹⁶⁴, S. Higashino⁸², E. Higón-Rodríguez¹⁷⁵, K. Hildebrand³⁷, E. Hill¹⁷⁷, J.C. Hill³², K.K. Hill²⁹, K.H. Hiller⁴⁶, S.J. Hillier²¹, M. Hils⁴⁸, I. Hinchliffe¹⁸, F. Hinterkeuser²⁴, M. Hirose¹³³, S. Hirose⁵², D. Hirschbuehl¹⁸³, B. Hiti⁹², O. Hladik¹⁴¹, D.R. Hlaluku^{33e}, X. Hoad⁵⁰, J. Hobbs¹⁵⁶, N. Hod¹⁸¹, M.C. Hodgkinson¹⁵⁰, A. Hoecker³⁶, F. Hoenig¹¹⁴, D. Hohn⁵², D. Hohov⁶⁵, T.R. Holmes³⁷, M. Holzbock¹¹⁴, L.B.A.H. Hommels³², S. Honda¹⁷⁰, T. Honda⁸², T.M. Hong¹³⁹, A. Hönle¹¹⁵, B.H. Hooberman¹⁷⁴, W.H. Hopkins⁶, Y. Horii¹¹⁷, P. Horn⁴⁸, L.A. Horyn³⁷, J.-Y. Hostachy⁵⁸, A. Hostiuc¹⁴⁹, S. Hou¹⁵⁹, A. Hoummada^{35a}, J. Howarth¹⁰¹, J. Hoya⁸⁹, M. Hrabovsky¹³¹, J. Hrdinka⁷⁷, I. Hristova¹⁹, J. Hrivnac⁶⁵, A. Hrynevich¹⁰⁹, T. Hryn'ova⁵, P.J. Hsu⁶⁴, S.-C. Hsu¹⁴⁹, Q. Hu²⁹, S. Hu^{60c}, Y. Huang^{15a}, Z. Hubacek¹⁴², F. Hubaut¹⁰², M. Huebner²⁴, F. Huegging²⁴, T.B. Huffman¹³⁵, M. Huhtinen³⁶, R.F.H. Hunter³⁴, P. Huo¹⁵⁶, A.M. Hupe³⁴, N. Huseynov^{80,ak}, J. Huston¹⁰⁷, J. Huth⁵⁹, R. Hyneman¹⁰⁶, S. Hyrych^{28a}, G. Iacobucci⁵⁴, G. Iakovidis²⁹, I. Ibragimov¹⁵², L. Iconomidou-Fayard⁶⁵, Z. Idrissi^{35e}, P. Iengo³⁶, R. Ignazzi⁴⁰, O. Igonkina^{120,ae,*}, R. Iguchi¹⁶⁴, T. Iizawa⁵⁴, Y. Ikegami⁸², M. Ikeno⁸², D. Iliadis¹⁶³, N. Ilic¹¹⁹, F. Iltzsche⁴⁸, G. Introzzi^{71a,71b}, M. Iodice^{75a}, K. Iordanidou^{169a}, V. Ippolito^{73a,73b}, M.F. Isacson¹⁷³, M. Ishino¹⁶⁴, M. Ishitsuka¹⁶⁶, W. Islam¹³⁰, C. Issever¹³⁵, S. Istin¹⁶¹, F. Ito¹⁷⁰, J.M. Iturbe Ponce^{63a}, R. Iuppa^{76a,76b}, A. Ivina¹⁸¹, H. Iwasaki⁸², J.M. Izen⁴³, V. Izzo^{70a}, P. Jacka¹⁴¹, P. Jackson¹, R.M. Jacobs²⁴, B.P. Jaeger¹⁵³, V. Jain², G. Jäkel¹⁸³, K.B. Jakobi¹⁰⁰, K. Jakobs⁵², S. Jakobsen⁷⁷, T. Jakoubek¹⁴¹, J. Jamieson⁵⁷, K.W. Janas^{84a}, R. Jansky⁵⁴, J. Janssen²⁴, M. Janus⁵³, P.A. Janus^{84a}, G. Jarlskog⁹⁷, N. Javadov^{80,ak}, T. Javůrek³⁶, M. Javurkova⁵², F. Jeanneau¹⁴⁵, L. Jeanty¹³², J. Jejelava^{160a,al}, A. Jelinskas¹⁷⁹, P. Jenni^{52,c}, J. Jeong⁴⁶, N. Jeong⁴⁶, S. Jézéquel⁵, H. Ji¹⁸², J. Jia¹⁵⁶, H. Jiang⁷⁹, Y. Jiang^{60a}, Z. Jiang^{154,s}, S. Jiggins⁵², F.A. Jimenez Morales³⁸, J. Jimenez Pena¹⁷⁵, S. Jin^{15c}, A. Jinaru^{27b}, O. Jinnouchi¹⁶⁶, H. Jivan^{33e}, P. Johansson¹⁵⁰, K.A. Johns⁷, C.A. Johnson⁶⁶, K. Jon-And^{45a,45b}, R.W.L. Jones⁹⁰, S.D. Jones¹⁵⁷, S. Jones⁷, T.J. Jones⁹¹, J. Jongmanns^{61a}, P.M. Jorge^{140a}, J. Jovicevic³⁶, X. Ju¹⁸, J.J. Jungbunrath¹¹⁵, A. Juste Rozas^{14,ac}, A. Kaczmarska⁸⁵, M. Kado^{73a,73b}, H. Kagan¹²⁷, M. Kagan¹⁵⁴, C. Kahra¹⁰⁰, T. Kaji¹⁸⁰, E. Kajomovitz¹⁶¹, C.W. Kalderon⁹⁷, A. Kaluza¹⁰⁰, A. Kamenshchikov¹²³, L. Kanjir⁹², Y. Kano¹⁶⁴, V.A. Kantserov¹¹², J. Kanzaki⁸², L.S. Kaplan¹⁸², D. Kar^{33e}, M.J. Kareem^{169b}, S.N. Karpov⁸⁰, Z.M. Karpova⁸⁰, V. Kartvelishvili⁹⁰, A.N. Karyukhin¹²³, L. Kashif¹⁸², R.D. Kass¹²⁷, A. Kastanas^{45a,45b}, Y. Kataoka¹⁶⁴, C. Kato^{60d,60c}, J. Katzy⁴⁶, K. Kawade⁸³, K. Kawagoe⁸⁸, T. Kawaguchi¹¹⁷, T. Kawamoto¹⁶⁴, G. Kawamura⁵³, E.F. Kay¹⁷⁷, V.F. Kazanin^{122b,122a}, R. Keeler¹⁷⁷, R. Kehoe⁴², J.S. Keller³⁴, E. Kellermann⁹⁷, D. Kelsey¹⁵⁷, J.J. Kempster²¹, J. Kendrick²¹, O. Kepka¹⁴¹, S. Kersten¹⁸³, B.P. Kerševan⁹², S. Ketabchi Haghighat¹⁶⁸, M. Khader¹⁷⁴, F. Khalil-Zada¹³, M. Khandoga¹⁴⁵, A. Khanov¹³⁰, A.G. Kharlamov^{122b,122a}, T. Kharlamova^{122b,122a}, E.E. Khoda¹⁷⁶,

A. Khodinov¹⁶⁷, T.J. Khoo⁵⁴, E. Khramov⁸⁰, J. Khubua^{160b}, S. Kido⁸³, M. Kiehn⁵⁴, C.R. Kilby⁹⁴,
 Y.K. Kim³⁷, N. Kimura^{67a,67c}, O.M. Kind¹⁹, B.T. King^{91,*}, D. Kirchmeier⁴⁸, J. Kirk¹⁴⁴, A.E. Kiryunin¹¹⁵,
 T. Kishimoto¹⁶⁴, D.P. Kisliuk¹⁶⁸, V. Kitali⁴⁶, O. Kivernyk⁵, E. Kladiva^{28b,*}, T. Klapdor-Kleingrothaus⁵²,
 M. Klassen^{61a}, M.H. Klein¹⁰⁶, M. Klein⁹¹, U. Klein⁹¹, K. Kleinknecht¹⁰⁰, P. Klimek¹²¹, A. Klimentov²⁹,
 T. Klingl²⁴, T. Klioutchnikova³⁶, F.F. Klitzner¹¹⁴, P. Kluit¹²⁰, S. Kluth¹¹⁵, E. Kneringer⁷⁷,
 E.B.F.G. Knoops¹⁰², A. Knue⁵², D. Kobayashi⁸⁸, T. Kobayashi¹⁶⁴, M. Kobel⁴⁸, M. Kocian¹⁵⁴, P. Kodys¹⁴³,
 P.T. Koenig²⁴, T. Koffas³⁴, N.M. Köhler¹¹⁵, T. Koi¹⁵⁴, M. Kolb^{61b}, I. Koletsou⁵, T. Komarek¹³¹, T. Kondo⁸²,
 N. Kondrashova^{60c}, K. Köneke⁵², A.C. König¹¹⁹, T. Kono¹²⁶, R. Konoplich^{125,ar}, V. Konstantinides⁹⁵,
 N. Konstantinidis⁹⁵, B. Konya⁹⁷, R. Kopeliansky⁶⁶, S. Koperny^{84a}, K. Korcyl⁸⁵, K. Kordas¹⁶³, G. Koren¹⁶²,
 A. Korn⁹⁵, I. Korolkov¹⁴, E.V. Korolkova¹⁵⁰, N. Korotkova¹¹³, O. Kortner¹¹⁵, S. Kortner¹¹⁵, T. Kosek¹⁴³,
 V.V. Kostyukhin²⁴, A. Kotwal⁴⁹, A. Koulouris¹⁰, A. Kourkouveli-Charalampidi^{71a,71b}, C. Kourkoumelis⁹,
 E. Kourlitis¹⁵⁰, V. Kouskoura²⁹, A.B. Kowalewska⁸⁵, R. Kowalewski¹⁷⁷, C. Kozakai¹⁶⁴, W. Kozanecki¹⁴⁵,
 A.S. Kozhin¹²³, V.A. Kramarenko¹¹³, G. Kramberger⁹², D. Krasnopevtsev^{60a}, M.W. Krasny¹³⁶,
 A. Krasznahorkay³⁶, D. Krauss¹¹⁵, J.A. Kremer^{84a}, J. Kretzschmar⁹¹, P. Krieger¹⁶⁸, F. Krieter¹¹⁴,
 A. Krishnan^{61b}, K. Krizka¹⁸, K. Kroeninger⁴⁷, H. Kroha¹¹⁵, J. Kroll¹⁴¹, J. Kroll¹³⁷, J. Krstic¹⁶,
 U. Kruchonak⁸⁰, H. Krüger²⁴, N. Krumnack⁷⁹, M.C. Kruse⁴⁹, J.A. Krzysiak⁸⁵, T. Kubota¹⁰⁵,
 O. Kuchinskaia¹⁶⁷, S. Kudah^{4b}, D. Kuechler⁴⁶, J.T. Kuechler⁴⁶, S. Kuehn³⁶, A. Kugel^{61a}, T. Kuhl⁴⁶,
 V. Kukhtin⁸⁰, R. Kukla¹⁰², Y. Kulchitsky^{108,ao}, S. Kuleshov^{147d}, Y.P. Kulinich¹⁷⁴, M. Kuna⁵⁸, T. Kunigo⁸⁶,
 A. Kupco¹⁴¹, T. Kupfer⁴⁷, O. Kuprash⁵², H. Kurashige⁸³, L.L. Kurchaninov^{169a}, Y.A. Kurochkin¹⁰⁸,
 A. Kurova¹¹², M.G. Kurth^{15a,15d}, E.S. Kuwertz³⁶, M. Kuze¹⁶⁶, A.K. Kvam¹⁴⁹, J. Kvita¹³¹, T. Kwan¹⁰⁴,
 A. La Rosa¹¹⁵, L. La Rotonda^{41b,41a}, F. La Ruffa^{41b,41a}, C. Lacasta¹⁷⁵, F. Lacava^{73a,73b}, D.P.J. Lack¹⁰¹,
 H. Lacker¹⁹, D. Lacour¹³⁶, E. Ladygin⁸⁰, R. Lafaye⁵, B. Laforge¹³⁶, T. Lagouri^{33e}, S. Lai⁵³, S. Lammers⁶⁶,
 W. Lampl⁷, C. Lampoudis¹⁶³, E. Lançon²⁹, U. Landgraf⁵², M.P.J. Landon⁹³, M.C. Lanfermann⁵⁴,
 V.S. Lang⁴⁶, J.C. Lange⁵³, R.J. Langenberg³⁶, A.J. Lankford¹⁷², F. Lanni²⁹, K. Lantzsck²⁴, A. Lanza^{71a},
 A. Lapertosa^{55b,55a}, S. Laplace¹³⁶, J.F. Laporte¹⁴⁵, T. Lari^{69a}, F. Lasagni Manghi^{23b,23a}, M. Lassnig³⁶,
 T.S. Lau^{63a}, A. Laudrain⁶⁵, A. Laurier³⁴, M. Lavorgna^{70a,70b}, M. Lazzaroni^{69a,69b}, B. Le¹⁰⁵,
 E. Le Guirriec¹⁰², M. LeBlanc⁷, T. LeCompte⁶, F. Ledroit-Guillon⁵⁸, C.A. Lee²⁹, G.R. Lee¹⁷, L. Lee⁵⁹,
 S.C. Lee¹⁵⁹, S.J. Lee³⁴, B. Lefebvre^{169a}, M. Lefebvre¹⁷⁷, F. Legger¹¹⁴, C. Leggett¹⁸, K. Lehmann¹⁵³,
 N. Lehmann¹⁸³, G. Lehmann Miotto³⁶, W.A. Leight⁴⁶, A. Leisos^{163,aa}, M.A.L. Leite^{81c}, C.E. Leitgeb¹¹⁴,
 R. Leitner¹⁴³, D. Lellouch^{181,*}, K.J.C. Leney⁴², T. Lenz²⁴, B. Lenzi³⁶, R. Leone⁷, S. Leone^{72a},
 C. Leonidopoulos⁵⁰, A. Leopold¹³⁶, G. Lerner¹⁵⁷, C. Leroy¹¹⁰, R. Les¹⁶⁸, C.G. Lester³², M. Levchenko¹³⁸,
 J. Levêque⁵, D. Levin¹⁰⁶, L.J. Levinson¹⁸¹, D.J. Lewis²¹, B. Li^{15b}, B. Li¹⁰⁶, C-Q. Li^{60a}, F. Li^{60c}, H. Li^{60a},
 H. Li^{60b}, J. Li^{60c}, K. Li¹⁵⁴, L. Li^{60c}, M. Li^{15a,15d}, Q. Li^{15a,15d}, Q.Y. Li^{60a}, S. Li^{60d,60c}, X. Li⁴⁶, Y. Li⁴⁶,
 Z. Li^{60b}, Z. Liang^{15a}, B. Liberti^{74a}, A. Liblong¹⁶⁸, K. Lie^{63c}, S. Liem¹²⁰, C.Y. Lin³², K. Lin¹⁰⁷, T.H. Lin¹⁰⁰,
 R.A. Linck⁶⁶, J.H. Lindon²¹, A.L. Lioni⁵⁴, E. Lipeles¹³⁷, A. Lipniacka¹⁷, M. Lisovyi^{61b}, T.M. Liss^{174,ay},
 A. Lister¹⁷⁶, A.M. Litke¹⁴⁶, J.D. Little⁸, B. Liu^{79,ah}, B.X. Liu⁶, H.B. Liu²⁹, H. Liu¹⁰⁶, J.B. Liu^{60a},
 J.K.K. Liu¹³⁵, K. Liu¹³⁶, M. Liu^{60a}, P. Liu¹⁸, Y. Liu^{15a,15d}, Y.L. Liu¹⁰⁶, Y.W. Liu^{60a}, M. Livan^{71a,71b},
 A. Lleres⁵⁸, J. Llorente Merino^{15a}, S.L. Lloyd⁹³, C.Y. Lo^{63b}, F. Lo Sterzo⁴², E.M. Lobodzinska⁴⁶, P. Loch⁷,
 S. Loffredo^{74a,74b}, T. Lohse¹⁹, K. Lohwasser¹⁵⁰, M. Lokajicek¹⁴¹, J.D. Long¹⁷⁴, R.E. Long⁹⁰, L. Longo³⁶,
 K.A. Looper¹²⁷, J.A. Lopez^{147d}, I. Lopez Paz¹⁰¹, A. Lopez Solis¹⁵⁰, J. Lorenz¹¹⁴, N. Lorenzo Martinez⁵,
 M. Losada^{22a}, P.J. Lösel¹¹⁴, A. Lösle⁵², X. Lou⁴⁶, X. Lou^{15a}, A. Lounis⁶⁵, J. Love⁶, P.A. Love⁹⁰,
 J.J. Lozano Bahilo¹⁷⁵, M. Lu^{60a}, Y.J. Lu⁶⁴, H.J. Lubatti¹⁴⁹, C. Luci^{73a,73b}, A. Lucotte⁵⁸, C. Luedtke⁵²,
 F. Luehring⁶⁶, I. Luise¹³⁶, L. Luminari^{73a}, B. Lund-Jensen¹⁵⁵, M.S. Lutz¹⁰³, D. Lynn²⁹, R. Lysak¹⁴¹,
 E. Lytken⁹⁷, F. Lyu^{15a}, V. Lyubushkin⁸⁰, T. Lyubushkina⁸⁰, H. Ma²⁹, L.L. Ma^{60b}, Y. Ma^{60b},
 G. Maccarrone⁵¹, A. Macchiolo¹¹⁵, C.M. Macdonald¹⁵⁰, J. Machado Miguens¹³⁷, D. Madaffari¹⁷⁵,
 R. Madar³⁸, W.F. Mader⁴⁸, N. Madysa⁴⁸, J. Maeda⁸³, K. Maekawa¹⁶⁴, S. Maeland¹⁷, T. Maeno²⁹,
 M. Maerker⁴⁸, A.S. Maevskiy¹¹³, V. Magerl⁵², N. Magini⁷⁹, D.J. Mahon³⁹, C. Maidantchik^{81b},
 T. Maier¹¹⁴, A. Maio^{140a,140b,140d}, K. Maj⁸⁵, O. Majersky^{28a}, S. Majewski¹³², Y. Makida⁸², N. Makovec⁶⁵,
 B. Malaescu¹³⁶, Pa. Malecki⁸⁵, V.P. Maleev¹³⁸, F. Malek⁵⁸, U. Mallik⁷⁸, D. Malon⁶, C. Malone³²,
 S. Maltezos¹⁰, S. Malyukov⁸⁰, J. Mamuzic¹⁷⁵, G. Mancini⁵¹, I. Mandić⁹²,
 L. Manhaes de Andrade Filho^{81a}, I.M. Maniatis¹⁶³, J. Manjarres Ramos⁴⁸, K.H. Mankinen⁹⁷, A. Mann¹¹⁴,
 A. Manousos⁷⁷, B. Mansoulie¹⁴⁵, I. Mantos¹⁶³, S. Manzoni¹²⁰, A. Marantis¹⁶³, G. Marceca³⁰,
 L. Marchese¹³⁵, G. Marchiori¹³⁶, M. Marcisovsky¹⁴¹, C. Marcon⁹⁷, C.A. Marin Tobon³⁶, M. Marjanovic³⁸,

Z. Marshall¹⁸, M.U.F. Martensson¹⁷³, S. Marti-Garcia¹⁷⁵, C.B. Martin¹²⁷, T.A. Martin¹⁷⁹, V.J. Martin⁵⁰, B. Martin dit Latour¹⁷, L. Martinelli^{75a,75b}, M. Martinez^{14,ac}, V.I. Martinez Outschoorn¹⁰³, S. Martin-Haugh¹⁴⁴, V.S. Martoiu^{27b}, A.C. Martyniuk⁹⁵, A. Marzin³⁶, S.R. Maschek¹¹⁵, L. Masetti¹⁰⁰, T. Mashimo¹⁶⁴, R. Mashinistov¹¹¹, J. Masik¹⁰¹, A.L. Maslennikov^{122b,122a}, L.H. Mason¹⁰⁵, L. Massa^{74a,74b}, P. Massarotti^{70a,70b}, P. Mastrandrea^{72a,72b}, A. Mastroberardino^{41b,41a}, T. Masubuchi¹⁶⁴, A. Matic¹¹⁴, P. Mättig²⁴, J. Maurer^{27b}, B. Maček⁹², D.A. Maximov^{122b,122a}, R. Mazini¹⁵⁹, I. Maznas¹⁶³, S.M. Mazza¹⁴⁶, S.P. Mc Kee¹⁰⁶, T.G. McCarthy¹¹⁵, L.I. McClymont⁹⁵, W.P. McCormack¹⁸, E.F. McDonald¹⁰⁵, J.A. Mcfayden³⁶, M.A. McKay⁴², K.D. McLean¹⁷⁷, S.J. McMahon¹⁴⁴, P.C. McNamara¹⁰⁵, C.J. McNicol¹⁷⁹, R.A. McPherson^{177,ai}, J.E. Mdhului^{33e}, Z.A. Meadows¹⁰³, S. Meehan¹⁴⁹, T. Megy⁵², S. Mehlhase¹¹⁴, A. Mehta⁹¹, T. Meideck⁵⁸, B. Meirose⁴³, D. Melini¹⁷⁵, B.R. Mellado Garcia^{33e}, J.D. Mellenthin⁵³, M. Melo^{28a}, F. Meloni⁴⁶, A. Melzer²⁴, S.B. Menary¹⁰¹, E.D. Mendes Gouveia^{140a,140e}, L. Meng³⁶, X.T. Meng¹⁰⁶, S. Menke¹¹⁵, E. Meoni^{41b,41a}, S. Mergelmeyer¹⁹, S.A.M. Merkt¹³⁹, C. Merlassino²⁰, P. Mermod⁵⁴, L. Merola^{70a,70b}, C. Meroni^{69a}, O. Meshkov^{113,111}, J.K.R. Meshreki¹⁵², A. Messina^{73a,73b}, J. Metcalfe⁶, A.S. Mete¹⁷², C. Meyer⁶⁶, J. Meyer¹⁶¹, J.-P. Meyer¹⁴⁵, H. Meyer Zu Theenhausen^{61a}, F. Miano¹⁵⁷, M. Michetti¹⁹, R.P. Middleton¹⁴⁴, L. Mijović⁵⁰, G. Mikenberg¹⁸¹, M. Mikesikova¹⁴¹, M. Mikuž⁹², H. Mildner¹⁵⁰, M. Milesi¹⁰⁵, A. Milic¹⁶⁸, D.A. Millar⁹³, D.W. Miller³⁷, A. Milov¹⁸¹, D.A. Milstead^{45a,45b}, R.A. Mina^{154,s}, A.A. Minaenko¹²³, M. Miñano Moya¹⁷⁵, I.A. Minashvili^{160b}, A.I. Mincer¹²⁵, B. Mindur^{84a}, M. Mineev⁸⁰, Y. Minegishi¹⁶⁴, Y. Ming¹⁸², L.M. Mir¹⁴, A. Mirto^{68a,68b}, K.P. Mistry¹³⁷, T. Mitani¹⁸⁰, J. Mitrevski¹¹⁴, V.A. Mitsou¹⁷⁵, M. Mittal^{60c}, A. Miucci²⁰, P.S. Miyagawa¹⁵⁰, A. Mizukami⁸², J.U. Mjörnmark⁹⁷, T. Mkrtchyan¹⁸⁵, M. Mlynarikova¹⁴³, T. Moa^{45a,45b}, K. Mochizuki¹¹⁰, P. Mogg⁵², S. Mohapatra³⁹, R. Moles-Valls²⁴, M.C. Mondragon¹⁰⁷, K. Mönig⁴⁶, J. Monk⁴⁰, E. Monnier¹⁰², A. Montalbano¹⁵³, J. Montejo Berlingen³⁶, M. Montella⁹⁵, F. Monticelli⁸⁹, S. Monzani^{69a}, N. Morange⁶⁵, D. Moreno^{22a}, M. Moreno Llácer³⁶, C. Moreno Martinez¹⁴, P. Morettini^{55b}, M. Morgenstern¹²⁰, S. Morgenstern⁴⁸, D. Mori¹⁵³, M. Morii⁵⁹, M. Morinaga¹⁸⁰, V. Morisbak¹³⁴, A.K. Morley³⁶, G. Mornacchi³⁶, A.P. Morris⁹⁵, L. Morvaj¹⁵⁶, P. Moschovakos³⁶, B. Moser¹²⁰, M. Mosidze^{160b}, T. Moskalets¹⁴⁵, H.J. Moss¹⁵⁰, J. Moss^{31,p}, K. Motohashi¹⁶⁶, E. Mountricha³⁶, E.J.W. Moyses¹⁰³, S. Muanza¹⁰², J. Mueller¹³⁹, R.S.P. Mueller¹¹⁴, D. Muenstermann⁹⁰, G.A. Mullier⁹⁷, J.L. Munoz Martinez¹⁴, F.J. Munoz Sanchez¹⁰¹, P. Murin^{28b}, W.J. Murray^{179,144}, A. Murrone^{69a,69b}, M. Muškinja¹⁸, C. Mwewa^{33a}, A.G. Myagkov^{123,as}, J. Myers¹³², M. Myska¹⁴², B.P. Nachman¹⁸, O. Nackenhorst⁴⁷, A. Nag Nag⁴⁸, K. Nagai¹³⁵, K. Nagano⁸², Y. Nagasaka⁶², M. Nagel⁵², E. Nagy¹⁰², A.M. Nairz³⁶, Y. Nakahama¹¹⁷, K. Nakamura⁸², T. Nakamura¹⁶⁴, I. Nakano¹²⁸, H. Nanjo¹³³, F. Napolitano^{61a}, R.F. Naranjo Garcia⁴⁶, R. Narayan⁴², D.I. Narrias Villar^{61a}, I. Naryshkin¹³⁸, T. Naumann⁴⁶, G. Navarro^{22a}, H.A. Neal^{106,*}, P.Y. Nechaeva¹¹¹, F. Nechansky⁴⁶, T.J. Neep²¹, A. Negri^{71a,71b}, M. Negrini^{23b}, C. Nellist⁵³, M.E. Nelson¹³⁵, S. Nemecek¹⁴¹, P. Nemethy¹²⁵, M. Nessi^{36,e}, M.S. Neubauer¹⁷⁴, M. Neumann¹⁸³, P.R. Newman²¹, Y.S. Ng¹⁹, Y.W.Y. Ng¹⁷², H.D.N. Nguyen¹⁰², T. Nguyen Manh¹¹⁰, E. Nibigira³⁸, R.B. Nickerson¹³⁵, R. Nicolaidou¹⁴⁵, D.S. Nielsen⁴⁰, J. Nielsen¹⁴⁶, N. Nikiforou¹¹, V. Nikolaenko^{123,as}, I. Nikolic-Audit¹³⁶, K. Nikolopoulos²¹, P. Nilsson²⁹, H.R. Nindhito⁵⁴, Y. Ninomiya⁸², A. Nisati^{73a}, N. Nishu^{60c}, R. Nisius¹¹⁵, I. Nitsche⁴⁷, T. Nitta¹⁸⁰, T. Nobe¹⁶⁴, Y. Noguchi⁸⁶, I. Nomidis¹³⁶, M.A. Nomura²⁹, M. Nordberg³⁶, N. Norjoharuddeen¹³⁵, T. Novak⁹², O. Novgorodova⁴⁸, R. Novotny¹⁴², L. Nozka¹³¹, K. Ntekas¹⁷², E. Nurse⁹⁵, F.G. Oakham^{34,ba}, H. Oberlack¹¹⁵, J. Ocariz¹³⁶, A. Ochi⁸³, I. Ochoa³⁹, J.P. Ochoa-Ricoux^{147a}, K. O'Connor²⁶, S. Oda⁸⁸, S. Odaka⁸², S. Oerdek⁵³, A. Ogrodnik^{84a}, A. Oh¹⁰¹, S.H. Oh⁴⁹, C.C. Ohm¹⁵⁵, H. Oide^{55b,55a}, M.L. Ojeda¹⁶⁸, H. Okawa¹⁷⁰, Y. Okazaki⁸⁶, Y. Okumura¹⁶⁴, T. Okuyama⁸², A. Olariu^{27b}, L.F. Oleiro Seabra^{140a}, S.A. Olivares Pino^{147a}, D. Oliveira Damazio²⁹, J.L. Oliver¹, M.J.R. Olsson¹⁷², A. Olszewski⁸⁵, J. Olszowska⁸⁵, D.C. O'Neil¹⁵³, A. Onofre^{140a,140e}, K. Onogi¹¹⁷, P.U.E. Onyisi¹¹, H. Oppen¹³⁴, M.J. Oreglia³⁷, G.E. Orellana⁸⁹, D. Orestano^{75a,75b}, N. Orlando¹⁴, R.S. Orr¹⁶⁸, V. O'Shea⁵⁷, R. Ospanov^{60a}, G. Otero y Garzon³⁰, H. Otono⁸⁸, M. Ouchrif^{35d}, J. Ouellette²⁹, F. Ould-Saada¹³⁴, A. Ouraou^{145,*}, Q. Ouyang^{15a}, M. Owen⁵⁷, R.E. Owen²¹, V.E. Ozcan^{12c}, N. Ozturk⁸, J. Pacalt¹³¹, H.A. Pacey³², K. Pachal⁴⁹, A. Pacheco Pages¹⁴, C. Padilla Aranda¹⁴, S. Pagan Griso¹⁸, M. Paganini¹⁸⁴, G. Palacino⁶⁶, S. Palazzo⁵⁰, S. Palestini³⁶, M. Palka^{84b}, D. Pallin³⁸, I. Panagoulas¹⁰, C.E. Pandini³⁶, J.G. Panduro Vazquez⁹⁴, P. Pani⁴⁶, G. Panizzo^{67a,67c}, L. Paolozzi⁵⁴, C. Papadatos¹¹⁰, K. Papageorgiou^{9,i}, A. Paramonov⁶, D. Paredes Hernandez^{63b}, S.R. Paredes Saenz¹³⁵, B. Parida¹⁶⁷, T.H. Park¹⁶⁸, A.J. Parker⁹⁰, M.A. Parker³², F. Parodi^{55b,55a}, E.W. Parrish¹²¹, J.A. Parsons³⁹, U. Parzefall⁵²,

L. Pascual Dominguez ¹³⁶, V.R. Pascuzzi ¹⁶⁸, J.M.P. Pasner ¹⁴⁶, E. Pasqualucci ^{73a}, S. Passaggio ^{55b}, F. Pastore ⁹⁴, P. Pasuwan ^{45a,45b}, S. Pataraja ¹⁰⁰, J.R. Pater ¹⁰¹, A. Pathak ¹⁸², T. Pauly ³⁶, B. Pearson ¹¹⁵, M. Pedersen ¹³⁴, L. Pedraza Diaz ¹¹⁹, R. Pedro ^{140a}, T. Peiffer ⁵³, S.V. Peleganchuk ^{122b,122a}, O. Penc ¹⁴¹, H. Peng ^{60a}, B.S. Peralva ^{81a}, M.M. Perego ⁶⁵, A.P. Pereira Peixoto ^{140a}, D.V. Perepelitsa ²⁹, F. Peri ¹⁹, L. Perini ^{69a,69b}, H. Pernegger ³⁶, S. Perrella ^{70a,70b}, K. Peters ⁴⁶, R.F.Y. Peters ¹⁰¹, B.A. Petersen ³⁶, T.C. Petersen ⁴⁰, E. Petit ¹⁰², A. Petridis ¹, C. Petridou ¹⁶³, M. Petrov ¹³⁵, F. Petrucci ^{75a,75b}, M. Pettee ¹⁸⁴, N.E. Pettersson ¹⁰³, K. Petukhova ¹⁴³, A. Peyaud ¹⁴⁵, R. Pezoa ^{147d}, L. Pezzotti ^{71a,71b}, T. Pham ¹⁰⁵, F.H. Phillips ¹⁰⁷, P.W. Phillips ¹⁴⁴, M.W. Phipps ¹⁷⁴, G. Piacquadio ¹⁵⁶, E. Pianori ¹⁸, A. Picazio ¹⁰³, R.H. Pickles ¹⁰¹, R. Piegaia ³⁰, D. Pietreanu ^{27b}, J.E. Pilcher ³⁷, A.D. Pilkington ¹⁰¹, M. Pinamonti ^{74a,74b}, J.L. Pinfold ³, M. Pitt ¹⁸¹, L. Pizzimento ^{74a,74b}, M.-A. Pleier ²⁹, V. Pleskot ¹⁴³, E. Plotnikova ⁸⁰, D. Pluth ⁷⁹, P. Podberezko ^{122b,122a}, R. Poettgen ⁹⁷, R. Poggi ⁵⁴, L. Poggioli ⁶⁵, I. Pogrebnyak ¹⁰⁷, D. Pohl ²⁴, I. Pokharel ⁵³, G. Polesello ^{71a}, A. Poley ¹⁸, A. Policicchio ^{73a,73b}, R. Polifka ¹⁴³, A. Polini ^{23b}, C.S. Pollard ⁴⁶, V. Polychronakos ²⁹, D. Ponomarenko ¹¹², L. Pontecorvo ³⁶, S. Popa ^{27a}, G.A. Popeneciu ^{27d}, D.M. Portillo Quintero ⁵⁸, S. Pospisil ¹⁴², K. Potamianos ⁴⁶, I.N. Potrap ⁸⁰, C.J. Potter ³², H. Potti ¹¹, T. Poulsen ⁹⁷, J. Poveda ³⁶, T.D. Powell ¹⁵⁰, G. Pownall ⁴⁶, M.E. Pozo Astigarraga ³⁶, P. Pralavorio ¹⁰², S. Prell ⁷⁹, D. Price ¹⁰¹, M. Primavera ^{68a}, S. Prince ¹⁰⁴, M.L. Proffitt ¹⁴⁹, N. Proklova ¹¹², K. Prokofiev ^{63c}, F. Prokoshin ⁸⁰, S. Protopopescu ²⁹, J. Proudfoot ⁶, M. Przybycien ^{84a}, D. Pudzha ¹³⁸, A. Puri ¹⁷⁴, P. Puzo ⁶⁵, J. Qian ¹⁰⁶, Y. Qin ¹⁰¹, A. Quadt ⁵³, M. Queitsch-Maitland ⁴⁶, A. Qureshi ¹, P. Rados ¹⁰⁵, F. Ragusa ^{69a,69b}, G. Rahal ⁹⁸, J.A. Raine ⁵⁴, S. Rajagopalan ²⁹, A. Ramirez Morales ⁹³, K. Ran ^{15a,15d}, T. Rashid ⁶⁵, S. Raspopov ⁵, M.G. Ratti ^{69a,69b}, D.M. Rauch ⁴⁶, F. Rauscher ¹¹⁴, S. Rave ¹⁰⁰, B. Ravina ¹⁵⁰, I. Ravinovich ¹⁸¹, J.H. Rawling ¹⁰¹, M. Raymond ³⁶, A.L. Read ¹³⁴, N.P. Readioff ⁵⁸, M. Reale ^{68a,68b}, D.M. Rebutti ^{71a,71b}, A. Redelbach ¹⁷⁸, G. Redlinger ²⁹, K. Reeves ⁴³, L. Rehnisch ¹⁹, J. Reichert ¹³⁷, D. Reikher ¹⁶², A. Reiss ¹⁰⁰, A. Rej ¹⁵², C. Rembser ³⁶, M. Renda ^{27b}, M. Rescigno ^{73a}, S. Resconi ^{69a}, E.D. Resseguie ¹³⁷, S. Rettie ¹⁷⁶, E. Reynolds ²¹, O.L. Rezanova ^{122b,122a}, P. Reznicek ¹⁴³, E. Ricci ^{76a,76b}, R. Richter ¹¹⁵, S. Richter ⁴⁶, E. Richter-Was ^{84b}, O. Ricken ²⁴, M. Ridel ¹³⁶, P. Rieck ¹¹⁵, C.J. Riegel ¹⁸³, O. Rifki ⁴⁶, M. Rijssenbeek ¹⁵⁶, A. Rimoldi ^{71a,71b}, M. Rimoldi ⁴⁶, L. Rinaldi ^{23b}, G. Ripellino ¹⁵⁵, B. Ristić ⁹⁰, E. Ritsch ³⁶, I. Riu ¹⁴, J.C. Rivera Vergara ¹⁷⁷, F. Rizatdinova ¹³⁰, E. Rizvi ⁹³, C. Rizzi ³⁶, R.T. Roberts ¹⁰¹, S.H. Robertson ^{104,ai}, M. Robin ⁴⁶, D. Robinson ³², J.E.M. Robinson ⁴⁶, C.M. Robles Gajardo ^{147d}, A. Robson ⁵⁷, E. Rocco ¹⁰⁰, C. Roda ^{72a,72b}, S. Rodriguez Bosca ¹⁷⁵, A. Rodriguez Perez ¹⁴, D. Rodriguez Rodriguez ¹⁷⁵, A.M. Rodríguez Vera ^{169b}, S. Roe ³⁶, O. Røhne ¹³⁴, R. Röhrig ¹¹⁵, C.P.A. Roland ⁶⁶, J. Roloff ⁵⁹, A. Romaniouk ¹¹², M. Romano ^{23b,23a}, N. Rompotis ⁹¹, M. Ronzani ¹²⁵, L. Roos ¹³⁶, S. Rosati ^{73a}, K. Rosbach ⁵², G. Rosin ¹⁰³, B.J. Rosser ¹³⁷, E. Rossi ⁴⁶, E. Rossi ^{75a,75b}, E. Rossi ^{70a,70b}, L.P. Rossi ^{55b}, L. Rossini ^{69a,69b}, R. Rosten ¹⁴, M. Rotaru ^{27b}, J. Rothberg ¹⁴⁹, D. Rousseau ⁶⁵, G. Rovelli ^{71a,71b}, A. Roy ¹¹, D. Roy ^{33e}, A. Rozanov ¹⁰², Y. Rozen ¹⁶¹, X. Ruan ^{33e}, F. Rubbo ¹⁵⁴, F. Rühr ⁵², A. Ruiz-Martinez ¹⁷⁵, A. Rummler ³⁶, Z. Rurikova ⁵², N.A. Rusakovich ⁸⁰, H.L. Russell ¹⁰⁴, L. Rustige ^{38,47}, J.P. Rutherford ⁷, E.M. Rüttinger ^{46,l}, M. Rybar ³⁹, G. Rybkin ⁶⁵, A. Ryzhov ¹²³, G.F. Rzehorz ⁵³, P. Sabatini ⁵³, G. Sabato ¹²⁰, S. Sacerdoti ⁶⁵, H.F-W. Sadrozinski ¹⁴⁶, R. Sadykov ⁸⁰, F. Safai Tehrani ^{73a}, B. Safarzadeh Samani ¹⁵⁷, P. Saha ¹²¹, S. Saha ¹⁰⁴, M. Sahinsoy ^{61a}, A. Sahu ¹⁸³, M. Saimpert ⁴⁶, M. Saito ¹⁶⁴, T. Saito ¹⁶⁴, H. Sakamoto ¹⁶⁴, A. Sakharov ^{125,ar}, D. Salamani ⁵⁴, G. Salamanna ^{75a,75b}, J.E. Salazar Loyola ^{147d}, P.H. Sales De Bruin ¹⁷³, A. Salnikov ¹⁵⁴, J. Salt ¹⁷⁵, D. Salvatore ^{41b,41a}, F. Salvatore ¹⁵⁷, A. Salvucci ^{63a,63b,63c}, A. Salzburger ³⁶, J. Samarati ³⁶, D. Sammel ⁵², D. Sampsonidis ¹⁶³, D. Sampsonidou ¹⁶³, J. Sánchez ¹⁷⁵, A. Sanchez Pineda ^{67a,67c}, H. Sandaker ¹³⁴, C.O. Sander ⁴⁶, I.G. Sanderswood ⁹⁰, M. Sandhoff ¹⁸³, C. Sandoval ^{22a}, D.P.C. Sankey ¹⁴⁴, M. Sannino ^{55b,55a}, Y. Sano ¹¹⁷, A. Sansoni ⁵¹, C. Santoni ³⁸, H. Santos ^{140a,140b}, S.N. Santpur ¹⁸, A. Santra ¹⁷⁵, A. Saponov ⁸⁰, J.G. Saraiva ^{140a,140d}, O. Sasaki ⁸², K. Sato ¹⁷⁰, E. Sauvan ⁵, P. Savard ^{168,ba}, N. Savic ¹¹⁵, R. Sawada ¹⁶⁴, C. Sawyer ¹⁴⁴, L. Sawyer ^{96,ap}, C. Sbarra ^{23b}, A. Sbrizzi ^{23a}, T. Scanlon ⁹⁵, J. Schaarschmidt ¹⁴⁹, P. Schacht ¹¹⁵, B.M. Schachtner ¹¹⁴, D. Schaefer ³⁷, L. Schaefer ¹³⁷, J. Schaeffer ¹⁰⁰, S. Schaepe ³⁶, U. Schäfer ¹⁰⁰, A.C. Schaffer ⁶⁵, D. Schaile ¹¹⁴, R.D. Schamberger ¹⁵⁶, N. Scharmberg ¹⁰¹, V.A. Schegelsky ¹³⁸, D. Scheirich ¹⁴³, F. Schenck ¹⁹, M. Schernau ¹⁷², C. Schiavi ^{55b,55a}, S. Schier ¹⁴⁶, L.K. Schildgen ²⁴, Z.M. Schillaci ²⁶, E.J. Schioppa ³⁶, M. Schioppa ^{41b,41a}, K.E. Schleicher ⁵², S. Schlenker ³⁶, K.R. Schmidt-Sommerfeld ¹¹⁵, K. Schmieden ³⁶, C. Schmitt ¹⁰⁰, S. Schmitt ⁴⁶, S. Schmitz ¹⁰⁰, J.C. Schmoeckel ⁴⁶, U. Schnoor ⁵², L. Schoeffel ¹⁴⁵, A. Schoening ^{61b}, P.G. Scholer ⁵², E. Schopf ¹³⁵, M. Schott ¹⁰⁰, J.F.P. Schouwenberg ¹¹⁹, J. Schovancova ³⁶, S. Schramm ⁵⁴, F. Schroeder ¹⁸³, A. Schulte ¹⁰⁰,

H-C. Schultz-Coulon^{61a}, M. Schumacher⁵², B.A. Schumm¹⁴⁶, Ph. Schune¹⁴⁵, A. Schwartzman¹⁵⁴, T.A. Schwarz¹⁰⁶, Ph. Schwemling¹⁴⁵, R. Schwienhorst¹⁰⁷, A. Sciandra¹⁴⁶, G. Sciolla²⁶, M. Scodreggio⁴⁶, M. Scornajenghi^{41b,41a}, F. Scuri^{72a}, F. Scutti¹⁰⁵, L.M. Scyboz¹¹⁵, C.D. Sebastiani^{73a,73b}, P. Seema¹⁹, S.C. Seidel¹¹⁸, A. Seiden¹⁴⁶, T. Seiss³⁷, J.M. Seixas^{81b}, G. Sekhniaidze^{70a}, K. Sekhon¹⁰⁶, S.J. Sekula⁴², N. Semprini-Cesari^{23b,23a}, S. Sen⁴⁹, S. Senkin³⁸, C. Serfon⁷⁷, L. Serin⁶⁵, L. Serkin^{67a,67b}, M. Sessa^{60a}, H. Severini¹²⁹, T. Šfiligoj⁹², F. Sforza¹⁷¹, A. Sfyrla⁵⁴, E. Shabalina⁵³, J.D. Shahinian¹⁴⁶, N.W. Shaikh^{45a,45b}, D. Shaked Renous¹⁸¹, L.Y. Shan^{15a}, R. Shang¹⁷⁴, J.T. Shank²⁵, M. Shapiro¹⁸, A. Sharma¹³⁵, A.S. Sharma¹, P.B. Shatalov¹²⁴, K. Shaw¹⁵⁷, S.M. Shaw¹⁰¹, A. Shcherbakova¹³⁸, Y. Shen¹²⁹, N. Sherafati³⁴, A.D. Sherman²⁵, P. Sherwood⁹⁵, L. Shi^{159,ax}, S. Shimizu⁸², C.O. Shimmin¹⁸⁴, Y. Shimogama¹⁸⁰, M. Shimojima¹¹⁶, I.P.J. Shipsey¹³⁵, S. Shirabe⁸⁸, M. Shiyakova^{80,af}, J. Shlomi¹⁸¹, A. Shmeleva¹¹¹, M.J. Shochet³⁷, J. Shojaii¹⁰⁵, D.R. Shope¹²⁹, S. Shrestha¹²⁷, E.M. Shrif^{33e}, E. Shulga¹⁸¹, P. Sicho¹⁴¹, A.M. Sickles¹⁷⁴, P.E. Sidebo¹⁵⁵, E. Sideras Haddad^{33e}, O. Sidiropoulou³⁶, A. Sidoti^{23b,23a}, F. Siegert⁴⁸, Dj. Sijacki¹⁶, M.Jr. Silva¹⁸², M.V. Silva Oliveira^{81a}, S.B. Silverstein^{45a}, S. Simion⁶⁵, E. Simioni¹⁰⁰, R. Simoniello¹⁰⁰, S. Simsek^{12b}, P. Sinervo¹⁶⁸, V. Sinetckii^{113,111}, N.B. Sinev¹³², M. Sioli^{23b,23a}, I. Siral¹⁰⁶, S.Yu. Sivoklokov¹¹³, J. Sjölin^{45a,45b}, E. Skorda⁹⁷, P. Skubic¹²⁹, M. Slawinska⁸⁵, K. Sliwa¹⁷¹, R. Slovak¹⁴³, V. Smakhtin¹⁸¹, B.H. Smart¹⁴⁴, J. Smiesko^{28a}, N. Smirnov¹¹², S.Yu. Smirnov¹¹², Y. Smirnov¹¹², L.N. Smirnova^{113,x}, O. Smirnova⁹⁷, J.W. Smith⁵³, M. Smizanska⁹⁰, K. Smolek¹⁴², A. Smykiewicz⁸⁵, A.A. Snesev¹¹¹, H.L. Snoek¹²⁰, I.M. Snyder¹³², S. Snyder²⁹, R. Sobie^{177,ai}, A.M. Soffa¹⁷², A. Soffer¹⁶², A. Sogaard⁵⁰, F. Sohns⁵³, C.A. Solans Sanchez³⁶, E.Yu. Soldatov¹¹², U. Soldevila¹⁷⁵, A.A. Solodkov¹²³, A. Soloshenko⁸⁰, O.V. Solovyanov¹²³, V. Solovyev¹³⁸, P. Sommer¹⁵⁰, H. Son¹⁷¹, W. Song¹⁴⁴, W.Y. Song^{169b}, A. Sopczak¹⁴², F. Sopkova^{28b}, C.L. Sotiropoulou^{72a,72b}, S. Sottocornola^{71a,71b}, R. Soualah^{67a,67c,h}, A.M. Soukharev^{122b,122a}, D. South⁴⁶, S. Spagnolo^{68a,68b}, M. Spalla¹¹⁵, M. Spangenberg¹⁷⁹, F. Spanò⁹⁴, D. Sperlich⁵², T.M. Spieker^{61a}, R. Spighi^{23b}, G. Spigo³⁶, M. Spina¹⁵⁷, D.P. Spiteri⁵⁷, M. Spousta¹⁴³, A. Stabile^{69a,69b}, B.L. Stamas¹²¹, R. Stamen^{61a}, M. Stamenkovic¹²⁰, E. Stanecka⁸⁵, R.W. Stanek⁶, B. Stanislaus¹³⁵, M.M. Stanitzki⁴⁶, M. Stankaityte¹³⁵, B. Stapf¹²⁰, E.A. Starchenko¹²³, G.H. Stark¹⁴⁶, J. Stark⁵⁸, S.H. Stark⁴⁰, P. Staroba¹⁴¹, P. Starovoitov^{61a}, S. Stärz¹⁰⁴, R. Staszewski⁸⁵, G. Stavropoulos⁴⁴, M. Stegler⁴⁶, P. Steinberg²⁹, A.L. Steinhebel¹³², B. Stelzer¹⁵³, H.J. Stelzer¹³⁹, O. Stelzer-Chilton^{169a}, H. Stenzel⁵⁶, T.J. Stevenson¹⁵⁷, G.A. Stewart³⁶, M.C. Stockton³⁶, G. Stoica^{27b}, M. Stolarski^{140a}, P. Stolte⁵³, S. Stonjek¹¹⁵, A. Straessner⁴⁸, J. Strandberg¹⁵⁵, S. Strandberg^{45a,45b}, M. Strauss¹²⁹, P. Strizenec^{28b}, R. Ströhmer¹⁷⁸, D.M. Strom¹³², R. Stroynowski⁴², A. Strubig⁵⁰, S.A. Stucci²⁹, B. Stugu¹⁷, J. Stupak¹²⁹, N.A. Styles⁴⁶, D. Su¹⁵⁴, S. Suchek^{61a}, V.V. Sulin¹¹¹, M.J. Sullivan⁹¹, D.M.S. Sultan⁵⁴, S. Sultansoy^{4c}, T. Sumida⁸⁶, S. Sun¹⁰⁶, X. Sun³, K. Suruliz¹⁵⁷, C.J.E. Suster¹⁵⁸, M.R. Sutton¹⁵⁷, S. Suzuki⁸², M. Svatos¹⁴¹, M. Swiatlowski³⁷, S.P. Swift², T. Swirski¹⁷⁸, A. Sydorenko¹⁰⁰, I. Sykora^{28a}, M. Sykora¹⁴³, T. Sykora¹⁴³, D. Ta¹⁰⁰, K. Tackmann^{46,ad}, J. Taenzer¹⁶², A. Taffard¹⁷², R. Tafirout^{169a}, H. Takai²⁹, R. Takashima⁸⁷, K. Takeda⁸³, T. Takeshita¹⁵¹, E.P. Takeva⁵⁰, Y. Takubo⁸², M. Talby¹⁰², A.A. Talyshev^{122b,122a}, N.M. Tamir¹⁶², J. Tanaka¹⁶⁴, M. Tanaka¹⁶⁶, R. Tanaka⁶⁵, S. Tapia Araya¹⁷⁴, S. Tapprogge¹⁰⁰, A. Tarek Abouelfadl Mohamed¹³⁶, S. Tarem¹⁶¹, G. Tarna^{27b,d}, G.F. Tartarelli^{69a}, P. Tas¹⁴³, M. Tasevsky¹⁴¹, T. Tashiro⁸⁶, E. Tassi^{41b,41a}, A. Tavares Delgado^{140a,140b}, Y. Tayalati^{35e}, A.J. Taylor⁵⁰, G.N. Taylor¹⁰⁵, W. Taylor^{169b}, A.S. Tee⁹⁰, R. Teixeira De Lima¹⁵⁴, P. Teixeira-Dias⁹⁴, H. Ten Kate³⁶, J.J. Teoh¹²⁰, S. Terada⁸², K. Terashi¹⁶⁴, J. Terron⁹⁹, S. Terzo¹⁴, M. Testa⁵¹, R.J. Teuscher^{168,ai}, S.J. Thais¹⁸⁴, T. Theveneaux-Pelzer⁴⁶, F. Thiele⁴⁰, D.W. Thomas⁹⁴, J.O. Thomas⁴², J.P. Thomas²¹, A.S. Thompson⁵⁷, P.D. Thompson²¹, L.A. Thomsen¹⁸⁴, E. Thomson¹³⁷, E.J. Thorpe⁹³, Y. Tian³⁹, R.E. Ticse Torres⁵³, V.O. Tikhomirov^{111,at}, Yu.A. Tikhonov^{122b,122a}, S. Timoshenko¹¹², P. Tipton¹⁸⁴, S. Tisserant¹⁰², K. Todome^{23b,23a}, S. Todorova-Nova⁵, S. Todt⁴⁸, J. Tojo⁸⁸, S. Tokár^{28a}, K. Tokushuku⁸², E. Tolley¹²⁷, K.G. Tomiwa^{33e}, M. Tomoto¹¹⁷, L. Tompkins^{154,s}, B. Tong⁵⁹, P. Tornambe¹⁰³, E. Torrence¹³², H. Torres⁴⁸, E. Torró Pastor¹⁴⁹, C. Tosciri¹³⁵, J. Toth^{102,ag}, D.R. Tovey¹⁵⁰, A. Traeet¹⁷, C.J. Treado¹²⁵, T. Trefzger¹⁷⁸, F. Tresoldi¹⁵⁷, A. Tricoli²⁹, I.M. Trigger^{169a}, S. Trincaz-Duvoid¹³⁶, W. Trischuk¹⁶⁸, B. Trocmé⁵⁸, A. Trofymov¹⁴⁵, C. Troncon^{69a}, M. Trovatelli¹⁷⁷, F. Trovato¹⁵⁷, L. Truong^{33c}, M. Trzebinski⁸⁵, A. Trzupek⁸⁵, F. Tsai⁴⁶, J.C-L. Tseng¹³⁵, P.V. Tsiarehka^{108,ao}, A. Tsirigotis¹⁶³, N. Tsirintanis⁹, V. Tsiskaridze¹⁵⁶, E.G. Tskhadadze^{160a}, M. Tsopoulou¹⁶³, I.I. Tsukerman¹²⁴, V. Tsulaia¹⁸, S. Tsuno⁸², D. Tsybychev¹⁵⁶, Y. Tu^{63b}, A. Tudorache^{27b}, V. Tudorache^{27b}, T.T. Tulbure^{27a}, A.N. Tuna⁵⁹, S. Turchikhin⁸⁰, D. Turgeman¹⁸¹, I. Turk Cakir^{4b,y}, R.J. Turner²¹,

R. Turra^{69a}, P.M. Tuts³⁹, S. Tzamarias¹⁶³, E. Tzovara¹⁰⁰, G. Uccielli⁴⁷, K. Uchida¹⁶⁴, I. Ueda⁸², M. Ughetto^{45a,45b}, F. Ukegawa¹⁷⁰, G. Unal³⁶, A. Undrus²⁹, G. Unel¹⁷², F.C. Ungaro¹⁰⁵, Y. Unno⁸², K. Uno¹⁶⁴, J. Urban^{28b}, P. Urquijo¹⁰⁵, G. Usai⁸, J. Usui⁸², Z. Uysal^{12d}, L. Vacavant¹⁰², V. Vacek¹⁴², B. Vachon¹⁰⁴, K.O.H. Vadla¹³⁴, A. Vaidya⁹⁵, C. Valderanis¹¹⁴, E. Valdes Santurio^{45a,45b}, M. Valente⁵⁴, S. Valentineti^{23b,23a}, A. Valero¹⁷⁵, L. Valéry⁴⁶, R.A. Vallance²¹, A. Vallier³⁶, J.A. Valls Ferrer¹⁷⁵, T.R. Van Daalen¹⁴, P. Van Gemmeren⁶, I. Van Vulpen¹²⁰, M. Vanadia^{74a,74b}, W. Vandelli³⁶, A. Vaniachine¹⁶⁷, D. Vannicola^{73a,73b}, R. Vari^{73a}, E.W. Varnes⁷, C. Varni^{55b,55a}, T. Varol⁴², D. Varouchas⁶⁵, K.E. Varvell¹⁵⁸, M.E. Vasile^{27b}, G.A. Vasquez¹⁷⁷, J.G. Vasquez¹⁸⁴, F. Vazeille³⁸, D. Vazquez Furelos¹⁴, T. Vazquez Schroeder³⁶, J. Veatch⁵³, V. Vecchio^{75a,75b}, M.J. Veen¹²⁰, L.M. Veloce¹⁶⁸, F. Veloso^{140a,140c}, S. Veneziano^{73a}, A. Ventura^{68a,68b}, N. Venturi³⁶, A. Verbytskyi¹¹⁵, V. Vercesi^{71a}, M. Verducci^{75a,75b}, C.M. Vergel Infante⁷⁹, C. Vergis²⁴, W. Verkerke¹²⁰, A.T. Vermeulen¹²⁰, J.C. Vermeulen¹²⁰, M.C. Vetterli^{153,ba}, N. Viaux Maira^{147d}, M. Vicente Barreto Pinto⁵⁴, T. Vickey¹⁵⁰, O.E. Vickey Boeriu¹⁵⁰, G.H.A. Viehhauser¹³⁵, L. Vigani¹³⁵, M. Villa^{23b,23a}, M. Villaplana Perez^{69a,69b}, E. Vilucchi⁵¹, M.G. Vincter³⁴, V.B. Vinogradov⁸⁰, A. Vishwakarma⁴⁶, C. Vittori^{23b,23a}, I. Vivarelli¹⁵⁷, M. Vogel¹⁸³, P. Vokac¹⁴², S.E. von Buddenbrock^{33e}, E. Von Toerne²⁴, V. Vorobel¹⁴³, K. Vorobev¹¹², M. Vos¹⁷⁵, J.H. Vossebeld⁹¹, M. Vozak¹⁰¹, N. Vranjes¹⁶, M. Vranjes Milosavljevic¹⁶, V. Vrba¹⁴², M. Vreeswijk¹²⁰, R. Vuillermet³⁶, I. Vukotic³⁷, P. Wagner²⁴, W. Wagner¹⁸³, J. Wagner-Kuhr¹¹⁴, S. Wahdan¹⁸³, H. Wahlberg⁸⁹, K. Wakamiya⁸³, V.M. Walbrecht¹¹⁵, J. Walder⁹⁰, R. Walker¹¹⁴, S.D. Walker⁹⁴, W. Walkowiak¹⁵², V. Wallangen^{45a,45b}, A.M. Wang⁵⁹, C. Wang^{60b}, F. Wang¹⁸², H. Wang¹⁸, H. Wang³, J. Wang¹⁵⁸, J. Wang^{61b}, P. Wang⁴², Q. Wang¹²⁹, R.-J. Wang¹⁰⁰, R. Wang^{60a}, R. Wang⁶, S.M. Wang¹⁵⁹, W.T. Wang^{60a}, W. Wang^{15c,aj}, W.X. Wang^{60a,aj}, Y. Wang^{60a,aj}, Z. Wang^{60c}, C. Wanotayaroj⁴⁶, A. Warburton¹⁰⁴, C.P. Ward³², D.R. Wardrope⁹⁵, N. Warrack⁵⁷, A. Washbrook⁵⁰, A.T. Watson²¹, M.F. Watson²¹, G. Watts¹⁴⁹, B.M. Waugh⁹⁵, A.F. Webb¹¹, S. Webb¹⁰⁰, C. Weber¹⁸⁴, M.S. Weber²⁰, S.A. Weber³⁴, S.M. Weber^{61a}, A.R. Weidberg¹³⁵, J. Weingarten⁴⁷, M. Weirich¹⁰⁰, C. Weiser⁵², P.S. Wells³⁶, T. Wenaus²⁹, T. Wengler³⁶, S. Wenig³⁶, N. Wermes²⁴, M.D. Werner⁷⁹, M. Wessels^{61a}, T.D. Weston²⁰, K. Whalen¹³², N.L. Whallon¹⁴⁹, A.M. Wharton⁹⁰, A.S. White¹⁰⁶, A. White⁸, M.J. White¹, D. Whiteson¹⁷², B.W. Whitmore⁹⁰, F.J. Wickens¹⁴⁴, W. Wiedenmann¹⁸², M. Wielers¹⁴⁴, N. Wieseotte¹⁰⁰, C. Wiglesworth⁴⁰, L.A.M. Wiik-Fuchs⁵², F. Wilk¹⁰¹, H.G. Wilkens³⁶, L.J. Wilkins⁹⁴, H.H. Williams¹³⁷, S. Williams³², C. Willis¹⁰⁷, S. Willocq¹⁰³, J.A. Wilson²¹, I. Wingerter-Seez⁵, E. Winkels¹⁵⁷, F. Winklmeier¹³², O.J. Winston¹⁵⁷, B.T. Winter⁵², M. Wittgen¹⁵⁴, M. Wobisch⁹⁶, A. Wolf¹⁰⁰, T.M.H. Wolf¹²⁰, R. Wolff¹⁰², R. Wölker¹³⁵, J. Wollrath⁵², M.W. Wolter⁸⁵, H. Wolters^{140a,140c}, V.W.S. Wong¹⁷⁶, N.L. Woods¹⁴⁶, S.D. Worm²¹, B.K. Wosiek⁸⁵, K.W. Woźniak⁸⁵, K. Wraight⁵⁷, S.L. Wu¹⁸², X. Wu⁵⁴, Y. Wu^{60a}, T.R. Wyatt¹⁰¹, B.M. Wynne⁵⁰, S. Xella⁴⁰, Z. Xi¹⁰⁶, L. Xia¹⁷⁹, D. Xu^{15a}, H. Xu^{60a,d}, L. Xu²⁹, T. Xu¹⁴⁵, W. Xu¹⁰⁶, Z. Xu^{60b}, Z. Xu¹⁵⁴, B. Yabsley¹⁵⁸, S. Yacoob^{33a}, K. Yajima¹³³, D.P. Yallup⁹⁵, D. Yamaguchi¹⁶⁶, Y. Yamaguchi¹⁶⁶, A. Yamamoto⁸², T. Yamanaka¹⁶⁴, F. Yamane⁸³, M. Yamatani¹⁶⁴, T. Yamazaki¹⁶⁴, Y. Yamazaki⁸³, Z. Yan²⁵, H.J. Yang^{60c,60d}, H.T. Yang¹⁸, S. Yang⁷⁸, X. Yang^{60b,58}, Y. Yang¹⁶⁴, W.-M. Yao¹⁸, Y.C. Yap⁴⁶, Y. Yasu⁸², E. Yatsenko^{60c,60d}, J. Ye⁴², S. Ye²⁹, I. Yeletsikh⁸⁰, M.R. Yexley⁹⁰, E. Yigitbasi²⁵, K. Yorita¹⁸⁰, K. Yoshihara¹³⁷, C.J.S. Young³⁶, C. Young¹⁵⁴, J. Yu⁷⁹, R. Yuan^{60b,j}, X. Yue^{61a}, S.P.Y. Yuen²⁴, B. Zabinski⁸⁵, G. Zacharis¹⁰, E. Zaffaroni⁵⁴, J. Zahreddine¹³⁶, A.M. Zaitsev^{123,as}, T. Zakareishvili^{160b}, N. Zakharchuk³⁴, S. Zambito⁵⁹, D. Zanzi³⁶, D.R. Zaripovas⁵⁷, S.V. Zeiřner⁴⁷, C. Zeitnitz¹⁸³, G. Zemaityte¹³⁵, J.C. Zeng¹⁷⁴, O. Zenin¹²³, T. Ženiř^{28a}, D. Zerwas⁶⁵, M. Zgubič¹³⁵, D.F. Zhang^{15b}, F. Zhang¹⁸², G. Zhang^{60a}, G. Zhang^{15b}, H. Zhang^{15c}, J. Zhang⁶, L. Zhang^{15c}, L. Zhang^{60a}, M. Zhang¹⁷⁴, R. Zhang^{60a}, R. Zhang²⁴, X. Zhang^{60b}, Y. Zhang^{15a,15d}, Z. Zhang^{63a}, Z. Zhang⁶⁵, P. Zhao⁴⁹, Y. Zhao^{60b}, Z. Zhao^{60a}, A. Zhemchugov⁸⁰, Z. Zheng¹⁰⁶, D. Zhong¹⁷⁴, B. Zhou¹⁰⁶, C. Zhou¹⁸², M.S. Zhou^{15a,15d}, M. Zhou¹⁵⁶, N. Zhou^{60c}, Y. Zhou⁷, C.G. Zhu^{60b}, H.L. Zhu^{60a}, H. Zhu^{15a}, J. Zhu¹⁰⁶, Y. Zhu^{60a}, X. Zhuang^{15a}, K. Zhukov¹¹¹, V. Zhulanov^{122b,122a}, D. Zieminska⁶⁶, N.I. Zimine⁸⁰, S. Zimmermann⁵², Z. Zinonos¹¹⁵, M. Ziolkowski¹⁵², L. Živković¹⁶, G. Zobernig¹⁸², A. Zoccoli^{23b,23a}, K. Zoch⁵³, T.G. Zorbass¹⁵⁰, R. Zou³⁷, L. Zwalinski³⁶,

¹ Department of Physics, University of Adelaide, Adelaide; Australia² Physics Department, SUNY Albany, Albany NY; United States of America³ Department of Physics, University of Alberta, Edmonton AB; Canada⁴ (a) Department of Physics, Ankara University, Ankara; (b) Istanbul Aydin University, Application and Research Center for Advanced Studies, Istanbul; (c) Division of Physics, TOBB University of Economics and Technology, Ankara; Turkey⁵ LAPP, Université Grenoble Alpes, Université Savoie Mont Blanc, CNRS/IN2P3, Annecy; France⁶ High Energy Physics Division, Argonne National Laboratory, Argonne IL; United States of America

- ⁷ Department of Physics, University of Arizona, Tucson AZ; United States of America
⁸ Department of Physics, University of Texas at Arlington, Arlington TX; United States of America
⁹ Physics Department, National and Kapodistrian University of Athens, Athens; Greece
¹⁰ Physics Department, National Technical University of Athens, Zografou; Greece
¹¹ Department of Physics, University of Texas at Austin, Austin TX; United States of America
¹² (a) Bahcesehir University, Faculty of Engineering and Natural Sciences, Istanbul; (b) Istanbul Bilgi University, Faculty of Engineering and Natural Sciences, Istanbul; (c) Department of Physics, Bogazici University, Istanbul; (d) Department of Physics Engineering, Gaziantep University, Gaziantep; Turkey
¹³ Institute of Physics, Azerbaijan Academy of Sciences, Baku; Azerbaijan
¹⁴ Institut de Física d'Altes Energies (IFAE), Barcelona Institute of Science and Technology, Barcelona; Spain
¹⁵ (a) Institute of High Energy Physics, Chinese Academy of Sciences, Beijing; (b) Physics Department, Tsinghua University, Beijing; (c) Department of Physics, Nanjing University, Nanjing; (d) University of Chinese Academy of Science (UCAS), Beijing; China
¹⁶ Institute of Physics, University of Belgrade, Belgrade; Serbia
¹⁷ Department for Physics and Technology, University of Bergen, Bergen; Norway
¹⁸ Physics Division, Lawrence Berkeley National Laboratory and University of California, Berkeley CA; United States of America
¹⁹ Institut für Physik, Humboldt Universität zu Berlin, Berlin; Germany
²⁰ Albert Einstein Center for Fundamental Physics and Laboratory for High Energy Physics, University of Bern, Bern; Switzerland
²¹ School of Physics and Astronomy, University of Birmingham, Birmingham; United Kingdom
²² (a) Facultad de Ciencias y Centro de Investigaciones, Universidad Antonio Nariño, Bogotá; (b) Departamento de Física, Universidad Nacional de Colombia, Bogotá; Colombia
²³ (a) INFN Bologna and Università di Bologna, Dipartimento di Fisica; (b) INFN Sezione di Bologna; Italy
²⁴ Physikalisches Institut, Universität Bonn, Bonn; Germany
²⁵ Department of Physics, Boston University, Boston MA; United States of America
²⁶ Department of Physics, Brandeis University, Waltham MA; United States of America
²⁷ (a) Transilvania University of Brasov, Brasov; (b) Horia Hulubei National Institute of Physics and Nuclear Engineering, Bucharest; (c) Department of Physics, Alexandru Ioan Cuza University of Iasi, Iasi; (d) National Institute for Research and Development of Isotopic and Molecular Technologies, Physics Department, Cluj-Napoca; (e) University Politehnica Bucharest, Bucharest; (f) West University in Timisoara, Timisoara; Romania
²⁸ (a) Faculty of Mathematics, Physics and Informatics, Comenius University, Bratislava; (b) Department of Subnuclear Physics, Institute of Experimental Physics of the Slovak Academy of Sciences, Kosice; Slovak Republic
²⁹ Physics Department, Brookhaven National Laboratory, Upton NY; United States of America
³⁰ Departamento de Física, Universidad de Buenos Aires, Buenos Aires; Argentina
³¹ California State University, CA; United States of America
³² Cavendish Laboratory, University of Cambridge, Cambridge; United Kingdom
³³ (a) Department of Physics, University of Cape Town, Cape Town; (b) iThemba Labs, Western Cape; (c) Department of Mechanical Engineering Science, University of Johannesburg, Johannesburg; (d) University of South Africa, Department of Physics, Pretoria; (e) School of Physics, University of the Witwatersrand, Johannesburg; South Africa
³⁴ Department of Physics, Carleton University, Ottawa ON; Canada
³⁵ (a) Faculté des Sciences Ain Chock, Réseau Universitaire de Physique des Hautes Energies – Université Hassan II, Casablanca; (b) Faculté des Sciences, Université Ibn-Tofail, Kénitra; (c) Faculté des Sciences Semlalia, Université Cadi Ayyad, LPHEA, Marrakech; (d) Faculté des Sciences, Université Mohamed Premier and LPTPM, Oujda; (e) Faculté des sciences, Université Mohammed V, Rabat; Morocco
³⁶ CERN, Geneva; Switzerland
³⁷ Enrico Fermi Institute, University of Chicago, Chicago IL; United States of America
³⁸ LPC, Université Clermont Auvergne, CNRS/IN2P3, Clermont-Ferrand; France
³⁹ Nevis Laboratory, Columbia University, Irvington NY; United States of America
⁴⁰ Niels Bohr Institute, University of Copenhagen, Copenhagen; Denmark
⁴¹ (a) Dipartimento di Fisica, Università della Calabria, Rende; (b) INFN Gruppo Collegato di Cosenza, Laboratori Nazionali di Frascati; Italy
⁴² Physics Department, Southern Methodist University, Dallas TX; United States of America
⁴³ Physics Department, University of Texas at Dallas, Richardson TX; United States of America
⁴⁴ National Centre for Scientific Research "Demokritos", Agia Paraskevi; Greece
⁴⁵ (a) Department of Physics, Stockholm University; (b) Oskar Klein Centre, Stockholm; Sweden
⁴⁶ Deutsches Elektronen-Synchrotron DESY, Hamburg and Zeuthen; Germany
⁴⁷ Lehrstuhl für Experimentelle Physik IV, Technische Universität Dortmund, Dortmund; Germany
⁴⁸ Institut für Kern- und Teilchenphysik, Technische Universität Dresden, Dresden; Germany
⁴⁹ Department of Physics, Duke University, Durham NC; United States of America
⁵⁰ SUPA – School of Physics and Astronomy, University of Edinburgh, Edinburgh; United Kingdom
⁵¹ INFN e Laboratori Nazionali di Frascati, Frascati; Italy
⁵² Physikalisches Institut, Albert-Ludwigs-Universität Freiburg, Freiburg; Germany
⁵³ II. Physikalisches Institut, Georg-August-Universität Göttingen, Göttingen; Germany
⁵⁴ Département de Physique Nucléaire et Corpusculaire, Université de Genève, Genève; Switzerland
⁵⁵ (a) Dipartimento di Fisica, Università di Genova, Genova; (b) INFN Sezione di Genova; Italy
⁵⁶ II. Physikalisches Institut, Justus-Liebig-Universität Giessen, Giessen; Germany
⁵⁷ SUPA – School of Physics and Astronomy, University of Glasgow, Glasgow; United Kingdom
⁵⁸ LPSC, Université Grenoble Alpes, CNRS/IN2P3, Grenoble INP, Grenoble; France
⁵⁹ Laboratory for Particle Physics and Cosmology, Harvard University, Cambridge MA; United States of America
⁶⁰ (a) Department of Modern Physics and State Key Laboratory of Particle Detection and Electronics, University of Science and Technology of China, Hefei; (b) Institute of Frontier and Interdisciplinary Science and Key Laboratory of Particle Physics and Particle Irradiation (MOE), Shandong University, Qingdao; (c) School of Physics and Astronomy, Shanghai Jiao Tong University, KLPPAC-MoE, SKLPPC, Shanghai; (d) Tsung-Dao Lee Institute, Shanghai; China
⁶¹ (a) Kirchhoff-Institut für Physik, Ruprecht-Karls-Universität Heidelberg, Heidelberg; (b) Physikalisches Institut, Ruprecht-Karls-Universität Heidelberg, Heidelberg; Germany
⁶² Faculty of Applied Information Science, Hiroshima Institute of Technology, Hiroshima; Japan
⁶³ (a) Department of Physics, Chinese University of Hong Kong, Shatin, N.T., Hong Kong; (b) Department of Physics, University of Hong Kong, Hong Kong; (c) Department of Physics and Institute for Advanced Study, Hong Kong University of Science and Technology, Clear Water Bay, Kowloon, Hong Kong; China
⁶⁴ Department of Physics, National Tsing Hua University, Hsinchu; Taiwan
⁶⁵ IJCLab, Université Paris-Saclay, CNRS/IN2P3, 91405, Orsay; France
⁶⁶ Department of Physics, Indiana University, Bloomington IN; United States of America
⁶⁷ (a) INFN Gruppo Collegato di Udine, Sezione di Trieste, Udine; (b) ICTP, Trieste; (c) Dipartimento Politecnico di Ingegneria e Architettura, Università di Udine, Udine; Italy
⁶⁸ (a) INFN Sezione di Lecce; (b) Dipartimento di Matematica e Fisica, Università del Salento, Lecce; Italy
⁶⁹ (a) INFN Sezione di Milano; (b) Dipartimento di Fisica, Università di Milano, Milano; Italy
⁷⁰ (a) INFN Sezione di Napoli; (b) Dipartimento di Fisica, Università di Napoli, Napoli; Italy
⁷¹ (a) INFN Sezione di Pavia; (b) Dipartimento di Fisica, Università di Pavia, Pavia; Italy
⁷² (a) INFN Sezione di Pisa; (b) Dipartimento di Fisica E. Fermi, Università di Pisa, Pisa; Italy
⁷³ (a) INFN Sezione di Roma; (b) Dipartimento di Fisica, Sapienza Università di Roma, Roma; Italy
⁷⁴ (a) INFN Sezione di Roma Tor Vergata; (b) Dipartimento di Fisica, Università di Roma Tor Vergata, Roma; Italy
⁷⁵ (a) INFN Sezione di Roma Tre; (b) Dipartimento di Matematica e Fisica, Università Roma Tre, Roma; Italy

- 76 ^(a) INFN-TIFPA; ^(b) Università degli Studi di Trento, Trento; Italy
- 77 Institut für Astro- und Teilchenphysik, Leopold-Franzens-Universität, Innsbruck; Austria
- 78 University of Iowa, Iowa City IA; United States of America
- 79 Department of Physics and Astronomy, Iowa State University, Ames IA; United States of America
- 80 Joint Institute for Nuclear Research, Dubna; Russia
- 81 ^(a) Departamento de Engenharia Elétrica, Universidade Federal de Juiz de Fora (UFJF), Juiz de Fora; ^(b) Universidade Federal do Rio De Janeiro COPPE/EE/IF, Rio de Janeiro; ^(c) Instituto de Física, Universidade de São Paulo, São Paulo; Brazil
- 82 KEK, High Energy Accelerator Research Organization, Tsukuba; Japan
- 83 Graduate School of Science, Kobe University, Kobe; Japan
- 84 ^(a) AGH University of Science and Technology, Faculty of Physics and Applied Computer Science, Krakow; ^(b) Marian Smoluchowski Institute of Physics, Jagiellonian University, Krakow; Poland
- 85 Institute of Nuclear Physics Polish Academy of Sciences, Krakow; Poland
- 86 Faculty of Science, Kyoto University, Kyoto; Japan
- 87 Kyoto University of Education, Kyoto; Japan
- 88 Research Center for Advanced Particle Physics and Department of Physics, Kyushu University, Fukuoka ; Japan
- 89 Instituto de Física La Plata, Universidad Nacional de La Plata and CONICET, La Plata; Argentina
- 90 Physics Department, Lancaster University, Lancaster; United Kingdom
- 91 Oliver Lodge Laboratory, University of Liverpool, Liverpool; United Kingdom
- 92 Department of Experimental Particle Physics, Jožef Stefan Institute and Department of Physics, University of Ljubljana, Ljubljana; Slovenia
- 93 School of Physics and Astronomy, Queen Mary University of London, London; United Kingdom
- 94 Department of Physics, Royal Holloway University of London, Egham; United Kingdom
- 95 Department of Physics and Astronomy, University College London, London; United Kingdom
- 96 Louisiana Tech University, Ruston LA; United States of America
- 97 Fysiska institutionen, Lunds universitet, Lund; Sweden
- 98 Centre de Calcul de l'Institut National de Physique Nucléaire et de Physique des Particules (IN2P3), Villeurbanne; France
- 99 Departamento de Física Teórica C-15 and CIAFF, Universidad Autónoma de Madrid, Madrid; Spain
- 100 Institut für Physik, Universität Mainz, Mainz; Germany
- 101 School of Physics and Astronomy, University of Manchester, Manchester; United Kingdom
- 102 CPPM, Aix-Marseille Université, CNRS/IN2P3, Marseille; France
- 103 Department of Physics, University of Massachusetts, Amherst MA; United States of America
- 104 Department of Physics, McGill University, Montreal QC; Canada
- 105 School of Physics, University of Melbourne, Victoria; Australia
- 106 Department of Physics, University of Michigan, Ann Arbor MI; United States of America
- 107 Department of Physics and Astronomy, Michigan State University, East Lansing MI; United States of America
- 108 B.I. Stepanov Institute of Physics, National Academy of Sciences of Belarus, Minsk; Belarus
- 109 Research Institute for Nuclear Problems of Byelorussian State University, Minsk; Belarus
- 110 Group of Particle Physics, University of Montreal, Montreal QC; Canada
- 111 P.N. Lebedev Physical Institute of the Russian Academy of Sciences, Moscow; Russia
- 112 National Research Nuclear University MEPhI, Moscow; Russia
- 113 D.V. Skobeltsyn Institute of Nuclear Physics, M.V. Lomonosov Moscow State University, Moscow; Russia
- 114 Fakultät für Physik, Ludwig-Maximilians-Universität München, München; Germany
- 115 Max-Planck-Institut für Physik (Werner-Heisenberg-Institut), München; Germany
- 116 Nagasaki Institute of Applied Science, Nagasaki; Japan
- 117 Graduate School of Science and Kobayashi-Maskawa Institute, Nagoya University, Nagoya; Japan
- 118 Department of Physics and Astronomy, University of New Mexico, Albuquerque NM; United States of America
- 119 Institute for Mathematics, Astrophysics and Particle Physics, Radboud University Nijmegen/Nikhef, Nijmegen; Netherlands
- 120 Nikhef National Institute for Subatomic Physics and University of Amsterdam, Amsterdam; Netherlands
- 121 Department of Physics, Northern Illinois University, DeKalb IL; United States of America
- 122 ^(a) Budker Institute of Nuclear Physics and NSU, SB RAS, Novosibirsk; ^(b) Novosibirsk State University Novosibirsk; Russia
- 123 Institute for High Energy Physics of the National Research Centre Kurchatov Institute, Protvino; Russia
- 124 Institute for Theoretical and Experimental Physics named by A.I. Alikhanov of National Research Centre "Kurchatov Institute", Moscow; Russia
- 125 Department of Physics, New York University, New York NY; United States of America
- 126 Ochanomizu University, Otsuka, Bunkyo-ku, Tokyo; Japan
- 127 Ohio State University, Columbus OH; United States of America
- 128 Faculty of Science, Okayama University, Okayama; Japan
- 129 Homer L. Dodge Department of Physics and Astronomy, University of Oklahoma, Norman OK; United States of America
- 130 Department of Physics, Oklahoma State University, Stillwater OK; United States of America
- 131 Palacký University, RCPTM, Joint Laboratory of Optics, Olomouc; Czech Republic
- 132 Institute for Fundamental Science, University of Oregon, Eugene, OR; United States of America
- 133 Graduate School of Science, Osaka University, Osaka; Japan
- 134 Department of Physics, University of Oslo, Oslo; Norway
- 135 Department of Physics, Oxford University, Oxford; United Kingdom
- 136 LPNHE, Sorbonne Université, Université de Paris, CNRS/IN2P3, Paris; France
- 137 Department of Physics, University of Pennsylvania, Philadelphia PA; United States of America
- 138 Konstantinov Nuclear Physics Institute of National Research Centre "Kurchatov Institute", PNPI, St. Petersburg; Russia
- 139 Department of Physics and Astronomy, University of Pittsburgh, Pittsburgh PA; United States of America
- 140 ^(a) Laboratório de Instrumentação e Física Experimental de Partículas – LIP, Lisboa; ^(b) Departamento de Física, Faculdade de Ciências, Universidade de Lisboa, Lisboa; ^(c) Departamento de Física, Universidade de Coimbra, Coimbra; ^(d) Centro de Física Nuclear da Universidade de Lisboa, Lisboa; ^(e) Departamento de Física, Universidade do Minho, Braga; ^(f) Departamento de Física Teórica y del Cosmos, Universidad de Granada, Granada (Spain); ^(g) Dep Física and CEFITEC de Faculdade de Ciências e Tecnologia, Universidade Nova de Lisboa, Caparica;
- ^(b) Instituto Superior Técnico, Universidade de Lisboa, Lisboa; Portugal
- 141 Institute of Physics of the Czech Academy of Sciences, Prague; Czech Republic
- 142 Czech Technical University in Prague, Prague; Czech Republic
- 143 Charles University, Faculty of Mathematics and Physics, Prague; Czech Republic
- 144 Particle Physics Department, Rutherford Appleton Laboratory, Didcot; United Kingdom
- 145 IRFU, CEA, Université Paris-Saclay, Gif-sur-Yvette; France
- 146 Santa Cruz Institute for Particle Physics, University of California Santa Cruz, Santa Cruz CA; United States of America
- 147 ^(a) Departamento de Física, Pontificia Universidad Católica de Chile, Santiago; ^(b) Universidad Andres Bello, Department of Physics, Santiago; ^(c) Instituto de Alta Investigación, Universidad de Tarapacá; ^(d) Departamento de Física, Universidad Técnica Federico Santa María, Valparaíso; Chile
- 148 Universidade Federal de São João del Rei (UFSJ), São João del Rei; Brazil
- 149 Department of Physics, University of Washington, Seattle WA; United States of America

- 150 Department of Physics and Astronomy, University of Sheffield, Sheffield; United Kingdom
 151 Department of Physics, Shinshu University, Nagano; Japan
 152 Department Physik, Universität Siegen, Siegen; Germany
 153 Department of Physics, Simon Fraser University, Burnaby BC; Canada
 154 SLAC National Accelerator Laboratory, Stanford CA; United States of America
 155 Physics Department, Royal Institute of Technology, Stockholm; Sweden
 156 Departments of Physics and Astronomy, Stony Brook University, Stony Brook NY; United States of America
 157 Department of Physics and Astronomy, University of Sussex, Brighton; United Kingdom
 158 School of Physics, University of Sydney, Sydney; Australia
 159 Institute of Physics, Academia Sinica, Taipei; Taiwan
 160 ^(a) E. Andronikashvili Institute of Physics, Iv. Javakhsishvili Tbilisi State University, Tbilisi; ^(b) High Energy Physics Institute, Tbilisi State University, Tbilisi; Georgia
 161 Department of Physics, Technion, Israel Institute of Technology, Haifa; Israel
 162 Raymond and Beverly Sackler School of Physics and Astronomy, Tel Aviv University, Tel Aviv; Israel
 163 Department of Physics, Aristotle University of Thessaloniki, Thessaloniki; Greece
 164 International Center for Elementary Particle Physics and Department of Physics, University of Tokyo, Tokyo; Japan
 165 Graduate School of Science and Technology, Tokyo Metropolitan University, Tokyo; Japan
 166 Department of Physics, Tokyo Institute of Technology, Tokyo; Japan
 167 Tomsk State University, Tomsk; Russia
 168 Department of Physics, University of Toronto, Toronto ON; Canada
 169 ^(a) TRIUMF, Vancouver BC; ^(b) Department of Physics and Astronomy, York University, Toronto ON; Canada
 170 Division of Physics and Tomonaga Center for the History of the Universe, Faculty of Pure and Applied Sciences, University of Tsukuba, Tsukuba; Japan
 171 Department of Physics and Astronomy, Tufts University, Medford MA; United States of America
 172 Department of Physics and Astronomy, University of California Irvine, Irvine CA; United States of America
 173 Department of Physics and Astronomy, University of Uppsala, Uppsala; Sweden
 174 Department of Physics, University of Illinois, Urbana IL; United States of America
 175 Instituto de Física Corpuscular (IFIC), Centro Mixto Universidad de Valencia – CSIC, Valencia; Spain
 176 Department of Physics, University of British Columbia, Vancouver BC; Canada
 177 Department of Physics and Astronomy, University of Victoria, Victoria BC; Canada
 178 Fakultät für Physik und Astronomie, Julius-Maximilians-Universität Würzburg, Würzburg; Germany
 179 Department of Physics, University of Warwick, Coventry; United Kingdom
 180 Waseda University, Tokyo; Japan
 181 Department of Particle Physics and Astrophysics, Weizmann Institute of Science, Rehovot; Israel
 182 Department of Physics, University of Wisconsin, Madison WI; United States of America
 183 Fakultät für Mathematik und Naturwissenschaften, Fachgruppe Physik, Bergische Universität Wuppertal, Wuppertal; Germany
 184 Department of Physics, Yale University, New Haven CT; United States of America
 185 Yerevan Physics Institute, Yerevan; Armenia

^a Also at Borough of Manhattan Community College, City University of New York, New York NY; United States of America.

^b Also at Centre for High Performance Computing, CSIR Campus, Rosebank, Cape Town; South Africa.

^c Also at CERN, Geneva; Switzerland.

^d Also at CPPM, Aix-Marseille Université, CNRS/IN2P3, Marseille; France.

^e Also at Département de Physique Nucléaire et Corpusculaire, Université de Genève, Genève; Switzerland.

^f Also at Departament de Física de la Universitat Autònoma de Barcelona, Barcelona; Spain.

^g Also at Departamento de Física, Instituto Superior Técnico, Universidade de Lisboa, Lisboa; Portugal.

^h Also at Department of Applied Physics and Astronomy, University of Sharjah, Sharjah; United Arab Emirates.

ⁱ Also at Department of Financial and Management Engineering, University of the Aegean, Chios; Greece.

^j Also at Department of Physics and Astronomy, Michigan State University, East Lansing MI; United States of America.

^k Also at Department of Physics and Astronomy, University of Louisville, Louisville, KY; United States of America.

^l Also at Department of Physics and Astronomy, University of Sheffield, Sheffield; United Kingdom.

^m Also at Department of Physics, Ben Gurion University of the Negev, Beer Sheva; Israel.

ⁿ Also at Department of Physics, California State University, East Bay; United States of America.

^o Also at Department of Physics, California State University, Fresno; United States of America.

^p Also at Department of Physics, California State University, Sacramento; United States of America.

^q Also at Department of Physics, King's College London, London; United Kingdom.

^r Also at Department of Physics, St. Petersburg State Polytechnical University, St. Petersburg; Russia.

^s Also at Department of Physics, Stanford University, Stanford CA; United States of America.

^t Also at Department of Physics, University of Adelaide, Adelaide; Australia.

^u Also at Department of Physics, University of Fribourg, Fribourg; Switzerland.

^v Also at Department of Physics, University of Michigan, Ann Arbor MI; United States of America.

^w Also at Dipartimento di Matematica, Informatica e Fisica, Università di Udine, Udine; Italy.

^x Also at Faculty of Physics, M.V. Lomonosov Moscow State University, Moscow; Russia.

^y Also at Giresun University, Faculty of Engineering, Giresun; Turkey.

^z Also at Graduate School of Science, Osaka University, Osaka; Japan.

^{aa} Also at Hellenic Open University, Patras; Greece.

^{ab} Also at IJCLab, Université Paris-Saclay, CNRS/IN2P3, 91405, Orsay; France.

^{ac} Also at Institutio Catalana de Recerca i Estudis Avancats, ICREA, Barcelona; Spain.

^{ad} Also at Institut für Experimentalphysik, Universität Hamburg, Hamburg; Germany.

^{ae} Also at Institute for Mathematics, Astrophysics and Particle Physics, Radboud University Nijmegen/Nikhef, Nijmegen; Netherlands.

^{af} Also at Institute for Nuclear Research and Nuclear Energy (INRNE) of the Bulgarian Academy of Sciences, Sofia; Bulgaria.

^{ag} Also at Institute for Particle and Nuclear Physics, Wigner Research Centre for Physics, Budapest; Hungary.

^{ah} Also at Institute of High Energy Physics, Chinese Academy of Sciences, Beijing; China.

^{ai} Also at Institute of Particle Physics (IPP); Canada.

^{aj} Also at Institute of Physics, Academia Sinica, Taipei; Taiwan.

^{ak} Also at Institute of Physics, Azerbaijan Academy of Sciences, Baku; Azerbaijan.

^{al} Also at Institute of Theoretical Physics, Iliia State University, Tbilisi; Georgia.

^{am} Also at Instituto de Física Teórica, IFT-UAM/CSIC, Madrid; Spain.

^{an} Also at Istanbul University, Dept. of Physics, Istanbul; Turkey.

- ^{ao} Also at Joint Institute for Nuclear Research, Dubna; Russia.
- ^{ap} Also at Louisiana Tech University, Ruston LA; United States of America.
- ^{aq} Also at LPNHE, Sorbonne Université, Université de Paris, CNRS/IN2P3, Paris; France.
- ^{ar} Also at Manhattan College, New York NY; United States of America.
- ^{as} Also at Moscow Institute of Physics and Technology State University, Dolgoprudny; Russia.
- ^{at} Also at National Research Nuclear University MEPhI, Moscow; Russia.
- ^{au} Also at Physics Department, An-Najah National University, Nablus; Palestine.
- ^{av} Also at Physics Dept, University of South Africa, Pretoria; South Africa.
- ^{aw} Also at Physikalisches Institut, Albert-Ludwigs-Universität Freiburg, Freiburg; Germany.
- ^{ax} Also at School of Physics, Sun Yat-sen University, Guangzhou; China.
- ^{ay} Also at The City College of New York, New York NY; United States of America.
- ^{az} Also at The Collaborative Innovation Center of Quantum Matter (CICQM), Beijing; China.
- ^{ba} Also at TRIUMF, Vancouver BC; Canada.
- ^{bb} Also at Università di Napoli Parthenope, Napoli; Italy.
- * Deceased.